

PROVIDING ACTIVE HAPTIC FEEDBACK IN TWO DIMENSIONS ON A
TOUCH SCREEN

by

Uğur Alican Alma

B.S., Manufacturing Engineering, Istanbul Technical University, 2012

Submitted to the Institute for Graduate Studies in
Science and Engineering in partial fulfillment of
the requirements for the degree of
Master of Science

Graduate Program in Mechanical Engineering
Boğaziçi University

2017

ACKNOWLEDGEMENTS

This work was supported by the Scientific and Technological Research Council of Turkey (TUBITAK, 113E601). I would like to express my gratitude to my supervisor Evren Samur for the great remarks and engagement through the learning process of this master thesis. Also, I would like to thank my co-advisor Assoc. Prof. Çetin Yılmaz for his precious comments and contributions on my master thesis. Besides my advisors, I would like to thank Halil Ibrahim Baştürk for his encouragement and insightful comments.

Furthermore, I would like to thank Gholamreza Ilkhani and Hüseyin Demircioğlu for supporting me for the long period of this research. Also, I am appreciate all members of Haptic and Robotic lab for sharing great moments with me. Lastly, I will always be grateful to my family, who have believed in me during the entire period of my master degree.

ABSTRACT

PROVIDING ACTIVE HAPTIC FEEDBACK IN TWO DIMENSIONS ON A TOUCH SCREEN

In this thesis, a two dimensional active electrostatic tactile display, which is capable of applying directional forces in two dimensions to a stationary finger, is analyzed. Directional forces are created using friction induced by electrostatic attraction. At the beginning, a shaker is used to move the tactile display in one dimension relative to the stationary finger in order to investigate the factors affecting active feedback such as relative displacement, frequency of excitation signal, and amplitude of the excitation signal. In the first step, minimum relative displacement necessary for directional force is examined. In the second step, lateral forces are measured for four distinct frequencies of electrostatic excitation. In the third step, the effect of the amplitude of excitation voltage is investigated. The results show the feasibility of creating active feedback on an electrostatic tactile display. Minimum relative displacement is found as 4 mm. Increasing frequency and amplitude of electrostatic signal lead to the higher value of the directional force. Following the set of experiments investigating the active feedback in one dimension, a planar mechanism is built to move the tactile display in two dimensions relative to a stationary finger. In order to clearly see the effect of orientation of the directional force with respect to the stationary finger, the tactile display is excited from 0 to 180 degrees with 45 degree increments. Besides, directional force is applied at 27 degrees to a stationary finger in a single experiment to investigate the feasibility of directional force at a small angle. The results show that active feedback is created in two dimensions on the electrostatic tactile display.

ÖZET

DOKUNMATİK EKРАН ÜZERİNDE İKİ BOYUTLU AKTİF GERİ BESLEME SAĞLANMASI

Günümüzde elektronik cihazlarda dokunmatik ekranların yaygın bir şekilde kullanıldığını görmekteyiz. Kullanıcıların, dokunmatik ekranlar aracılığıyla sanal nesnelere kurduğu ilişkinin tatminkar olmaması sebebiyle geri beslemelerin geliştirilebilmesi için araştırmalar yapılmaktadır. Yapılan araştırmalar, parmağın ekran üzerinde hareket ederken alınabilecek geri beslemelerin geliştirilmesi üzerine yoğunlaşmaktadır ve bu geri beslemeler, pasif geri besleme olarak adlandırılmaktadır. Öte yandan, parmağın ekran üzerinde sabit konumlandığı durumlarda da geri besleme alabilmesi için çalışmalar yapılmaya başlanmıştır ve bu geri beslemelere aktif geri besleme adı verilmektedir. Bu tezde, elektrostatik dokunmatik ekranlar üzerinde sabit duran bir parmağa uygulanan kuvvetin yön değişimi analiz edilmiştir. İki boyutlu kuvvetler, elektrostatik kuvvet ile sürtünmeyi kontrol ederek yaratılır. Başlangıçta, bağıl yer değiştirme, elektrostatik kuvvet sinyalinin frekansı ve bu sinyalin genliği gibi önemli faktörleri araştırmak için deneyler yapılmıştır. Sonuçlar, elektrostatik dokunmatik ekranlarda aktif geribesleme oluşumunu sağlayan parametrelerin etkilerini göstermektedir. Minimum bağıl yer değiştirme miktarı 4 mm olarak bulunmuştur. Elektrostatik sinyal frekansı ve genliğinin artması tek yönlü kuvvetin artmasına yol açtığı gözlemlenmiştir. Bir boyutta aktif geri beslemeyi araştıran deneylerin ardından, dokunmatik ekranı sabit duran parmağa göre iki boyutta hareket ettirebilmek için düzlemsel bir mekanizma tasarlanmıştır. Sabit duran parmağa göre tek yönlü kuvvetin yön değiştirebildiğini gözlemleyebilmek için, ekran 0 dereceden 180 dereceye kadar 45 derecelik artışlarla titreştirildi. Daha dar bir açıda iki boyutlu kuvvetin fizibilitesi araştırmak için, sabit duran parmağa 27 derecelik açı ile de kuvvet uygulandı. Sonuçlar, aktif geri beslemenin dokunmatik ekranda iki boyutta oluşturulduğunu göstermektedir.

TABLE OF CONTENTS

ACKNOWLEDGEMENTS	iii
ABSTRACT	iv
ÖZET	v
LIST OF FIGURES	viii
LIST OF TABLES	xiii
LIST OF SYMBOLS	xiv
LIST OF ACRONYMS/ABBREVIATIONS	xv
1. INTRODUCTION	1
1.1. Motivation	1
1.2. Purpose and Contributions	3
1.3. Objectives	4
2. LITERATURE REVIEW	5
2.1. Ultrasonic Vibration Method	6
2.2. Electro vibration Method	7
2.3. Tribology of Fingertip	11
3. METHODOLOGY	13
3.1. Experimental Setups	14
3.1.1. 1-DOF Experimental Setup	14
3.1.2. 2-DOF Experimental Setup	17
3.1.2.1. Centric slider crank mechanism	18
3.1.2.2. Artificial finger	30
3.2. Experimental Procedures	32
3.2.1. 1D Measurements	32
3.2.1.1. Relative displacement	32
3.2.1.2. Frequency of electrostatic excitation signal	33
3.2.1.3. Amplitude of electrostatic excitation signal	33
3.2.2. 2D Measurements	33
3.2.2.1. Directional forces at 27° and 45°	34
3.2.2.2. Orienting the directional force	35

4. EXPERIMENTAL RESULTS	37
4.1. Experimental Results of 1D Measurements	37
4.1.1. Minimum Displacement for Active Feedback	37
4.1.2. Effect of Frequency on Directional Force	37
4.1.3. Effect of Amplitude on Directional Force	38
4.2. Experimental Results of 2D Measurements	39
4.2.1. Directional Forces at 27° and 45°	39
4.2.2. Orienting the Directional Force	47
5. DISCUSSION	49
6. CONCLUSION	52
6.1. Outlook and Future Work	53
REFERENCES	56

LIST OF FIGURES

Figure 1.1.	Passive and active feedback illustration.	3
Figure 2.1.	A touch surface is vibrated at its resonant frequency using a piezo-electric actuator in the ultrasonic vibration method. Reprinted from [22].	6
Figure 2.2.	Layers of skin tissue. Reprinted from [22].	9
Figure 2.3.	The layers of the electrostatic tactile display. Reprinted from [29].	9
Figure 2.4.	The hysteresis loop of viscoelastic materials represents the energy dissipation during load-unload cycle.	12
Figure 3.1.	Input signals to create active feedback on an electrostatic tactile display. Periodic square wave excitation for electrostatic attraction is synchronized with the sinusoidal motion of the display.	14
Figure 3.2.	Illustration of the experimental setup used to measure lateral forces acting on the index finger.	15
Figure 3.3.	Control schematic of the 1-DOF experimental setup.	16
Figure 3.4.	Block diagram of the 1-DOF experimental setup.	16
Figure 3.5.	3D render of the 2-DOF mechanism which consists of two stepper motors, two slider crank mechanisms, a touch screen and a base. .	17
Figure 3.6.	The experimental setup for 2D measurements.	18

Figure 3.7.	Control schematic. a) Labview control panel with control blocks, b) stepper motor driver circuit, and c) square wave excitation signal with 20 ms delay.	19
Figure 3.8.	Block diagram of the 2-DOF experimental setup.	19
Figure 3.9.	Centric slider crank mechanism modeled in ADAMS.	20
Figure 3.10.	Free body diagrams of the centric slider crank mechanism. Mass of the coupler link, m_3 , is 0.03 kg, and its center of gravity is in the middle. The mass, m_4 which is 0.8 kg, corresponds to the total mass of the tactile display and the slider crank mechanism working along X axis. To calculate the friction force, F_f , the dynamic friction coefficient is 0.25 based on the data sheet.	21
Figure 3.11.	Velocity and acceleration profiles of the tactile display along X axis.	24
Figure 3.12.	Torque about crank shaft at 1 Hz of frequency.	25
Figure 3.13.	The calculated torque about crank shaft at 1 Hz of frequency in MATLAB. The dashed line shows the torque value without friction force on the linear guides.	26
Figure 3.14.	Torque about crank shaft at 5 Hz of frequency.	26
Figure 3.15.	The calculated torque about crank shaft at 5 Hz of frequency in MATLAB. The dashed line shows the torque value without friction force on the linear guides.	27
Figure 3.16.	Torque about crank shaft at 10 Hz of frequency.	27

Figure 3.17.	The calculated torque about crank shaft at 10 Hz of frequency in MATLAB. The dashed line shows the torque value without friction force on the linear guides.	28
Figure 3.18.	Torque about crank shaft at 25 Hz of frequency.	28
Figure 3.19.	Torque about crank shaft at 50 Hz of frequency.	29
Figure 3.20.	Torque-speed curve of the stepper motor (POLOLU, Nema 14) which was driven at 12 VDC.	29
Figure 3.21.	FFT is applied to torque values about crank shaft at frequency of 5 Hz. Harmonics of the input are seen at 10 Hz increments.	30
Figure 3.22.	Components of the artificial finger. The force sensor is attached to the artificial finger using strong double-sided tape.	31
Figure 3.23.	Directional force fields at 27 and 45 degree angles.	35
Figure 3.24.	Rotated directional force field in sequence.	36
Figure 4.1.	Measured lateral forces for three relative displacements when the electrostatic tactile display was driven by a 270 Hz and 397 V _{pp} square wave which was periodically enabled and disabled at 5 Hz. (Bottom) Synchronized input signals.	38
Figure 4.2.	Measured lateral forces for four electrostatic excitation frequencies. Blue line represents the condition that 397 V _{pp} square wave was periodically enabled and disabled at 5 Hz. The black dashed lines show the measurements when the electrostatic attraction was disabled.	39

Figure 4.3.	Measured lateral forces for three different voltage conditions when the electrostatic tactile display was driven by a 270 Hz square wave, which was periodically enabled and disabled at 5 Hz. The finger was electrically grounded for one of the 215 V_{pp} cases.	40
Figure 4.4.	Lateral forces measured along X axis when the tactile display was moved with 4 mm stroke. The top rectangular area show the lateral forces with an electrostatic force, while the bottom rectangular area and the rest show the lateral forces without an electrostatic force.	41
Figure 4.5.	Lateral forces measured along Y axis when the tactile display was moved with 4 mm stroke. The bottom rectangular area show the lateral forces with an electrostatic force, while the top rectangular area and the rest show the lateral forces without an electrostatic force.	42
Figure 4.6.	Lateral forces measured along Y axis when the tactile display was moved with 2 mm stroke for the 27 degree experiment. The bottom rectangular area show the lateral forces with an electrostatic force, while the top rectangular area and the rest show the lateral forces without an electrostatic force.	43
Figure 4.7.	Lateral forces measured along Y axis for the 27 degree experiment were passed through a low pass filter with a cut-off frequency of 30 Hz.	43
Figure 4.8.	Lateral forces measured along X axis for the 45 degree experiment were passed through a low pass filter with a cut-off frequency of 30 Hz.	44

Figure 4.9.	Selected areas in order to calculate the two mean kinetic friction coefficients and their standard errors when there is an electrostatic force and not.	45
Figure 4.10.	Frequency domain analysis when there is an electrostatic force with 4 mm stroke along X axis.	46
Figure 4.11.	Frequency domain analysis when there is not an electrostatic force with 4 mm stroke in X axis.	46
Figure 4.12.	Force values measured in X axis at 4 mm stroke when directional force rotates from 0 to 180 degree angles.	47
Figure 4.13.	Force values measured in X axis at 4 mm stroke when directional force rotates from 45 to 135 degree angles.	48

LIST OF TABLES

Table 3.1.	Maximum torque values [Nmm].	25
Table 3.2.	Electrical conductivity and elastic modulus of a bare finger and an artificial finger [59, 60, 61].	31

LIST OF SYMBOLS

a_{G3x}	Acceleration of coupler in X axis
a_{G3y}	Acceleration of coupler in Y axis
F_f	Friction force on linear guide
F	Electrostatic force
m_3	Mass of coupler link
m_4	Total mass of tactile display and the slider crank mechanism
l	Coupler length
r	Crank length
s	Stroke
T_{12}	Total torque about crank shaft
V_E	Excitation signal of the capacitive tactile display
V_S	Excitation signal of the shaker
μ	Kinetic friction coefficient of the linear guide
μ_k	Kinetic friction coefficient between the tactile display and the finger
μ_s	Static friction coefficient between the tactile display and the finger
ϕ	Angle between crank link and X axis
Θ	Angle between coupler link and X axis

LIST OF ACRONYMS/ABBREVIATIONS

AC	Alternating current
DAQ	Data acquisition card
FFT	Fast fourier transformation
NI	National instruments
LCD	Liquid crystal display
RC	Resistor and capacitor
RPM	Revolution per minute
VDC	Direct current voltage
1D	One dimensional
2D	Two dimensional
3D	Three dimensional
1-DOF	One degree of freedom
2-DOF	Two degrees of freedom

1. INTRODUCTION

1.1. Motivation

In the field of haptic technology, the main goal is to generate touch sensations of interaction between a human and a virtual environment or telerobotic system. This relatively new research area is rapidly emerging. Haptic technology is based on the basics of robotics, control theory and human skin properties as well as psychology. In the literature, haptics is related with perception via cutaneous (tactile) receptors and kinesthetic (force/position) sensations. Specifically, haptics is described as real and virtual touch sensations between humans, robots, telerobotic devices and virtual environments [1]. So far, haptic technology has been commercially used in entertainment, medical simulations, and electronic devices [2]. Haptic feedback is used to increase usability and realism in virtual environment by combining touch with vision and sound. We experience haptic technology in many of the consumer devices which are used in everyday life [1]. Thanks to devices and interfaces using this technology, it is possible to feel objects in virtual environments. As a result of research carried out since the beginning of 1990s, this technology began to be used in surgical robots, computer games and medical simulators [3].

Touch screens are among the main application areas of the haptic technology. There are two main examples of haptics in touch screens, one is the rumble effect in a game controller console and the reassuring touch vibration on smart phone dial pad [2]. However, smart phones, computers and electronic devices with touch screens providing tactile feedback either does not exist or its application is limited to simple vibrations, which is not satisfactory to convince users that their desired action is completed. For example, the reason why touch screen users often make typing mistakes is the insufficient localized tactile feedback they receive [4]. Therefore, Senseg and Nokia companies started applying this technology in their products [5, 6].

In order to feel texture and geometry of a virtual object, friction force between fingertip and touch screen should be modulated because feeling texture is related with roughness of the surface while feeling geometry is related with the unidirectional force. In the literature, there are two methods to modulate the friction force, which are ultrasonic vibration and electrovibration method. Basically, ultrasonic vibration method decreases the friction force by creating an air film layer between the fingertip and the surface. On the other hand, electrovibration method increases the friction force by attracting fingertip by electrostatic forces. Due to many downsides of ultrasonic vibration method, such as noise introduced due to mechanical actuation, electrovibration method is preferred in this study.

Up to present, variety of studies [7]–[8] have been done in passive haptic systems to investigate roughness modulation on tactile displays. In a passive haptic system, tactile feedback occurs if the finger moves on the haptic surface modulating friction force. The passive feedback systems, which have been used to date, are not satisfactory since although they enable to feel texture of virtual object, geometry of the object can not be felt with these systems. Also, if the finger is stationary, any feedback corresponding to a virtual object cannot be transmitted to the finger. However, tactile feedback would be transmitted if the touch screen moves with convenient frequency and amplitude to create friction force between finger and touchscreen. This phenomena is called active feedback. An illustration of active and passive feedback can be seen in Figure 1.1. In active feedback, the finger is stationary when the touch screen moves periodically above the LCD screen.

This thesis focuses on creating active feedback in simulated touch interactions to overcome typing mistakes. However, despite the fact that the active feedback has been experimented with the ultrasonic vibration method [9, 10] and electrovibration method [11, 12] before, generating a 2-DOF active feedback with electrovibration method has never been realized in the literature.

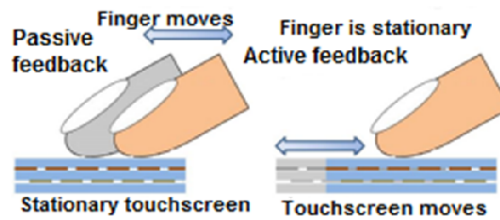


Figure 1.1. Passive and active feedback illustration.

1.2. Purpose and Contributions

This research is limited to haptic touch screens. The target area is the whole touch screen systems such as smartphones and tablets, in which tactile feedback is important. To feel virtual objects and their geometry on a touch screen, the friction force between fingertip and touchscreen should be controlled, which occurs when the finger moves laterally. In order to improve haptic feedback technology to create realistic physical interaction between a touchscreen and a user, active feedback is targeted. Contrary to a passive haptic system, active haptic system enables to feel virtual objects even if the fingertip is stationary, since, the required relative motion is provided by the movement of touchscreen with defined amplitude and frequency.

Electrovibration method is combined with mechanical actuation of the tactile display. For this purpose, a planar 2-DOF mechanism, is developed that two slider crank mechanisms actuated with step motors are considered in order to excite the tactile display in X and Y axes. As long as these planar mechanisms and electrostatic forces are acting with appropriate frequencies, which should be synchronized well with each other, an active tactile feedback is obtained. In this thesis, an active feedback in two dimensions is proposed on an electrostatic tactile display. Thus, combining mechanical actuation and electrovibration method is novel because this combination has not been used before for planar systems. In the literature, active feedback has been successfully demonstrated on ultrasonic surface haptic displays [10, 11]. Although Mullenbach *et al.*[12] used a similar approach to obtain 1-DOF active feedback, the method has been implemented in 2-DOF for the first time in the literature.

Consequently, active feedback system is aimed to be obtained properly via our experimental procedure. First step of this study proposes to demonstrate the feasibility of creating one degree of freedom (DOF) directional force on an electrostatic tactile display and investigating factors affecting active feedback such as relative displacement, frequency of excitation signal and amplitude of the excitation signal. In the second step, our work in one dimensional experimental setup is extended to two degree of freedom active feedback on an electrostatic tactile display. The expected result of experiments is to feel directional forces in 2D plane on electrostatic tactile display when the finger is stationary in contrast to a passive haptic system. With this thesis, innovative and practical recommendations are offered to remedy the shortcomings in the existing technology.

1.3. Objectives

In order to provide rich haptic feedback on touch screens, our goal is to develop a novel technology, combining mechanical actuation and electrovibration method for active feedback. The specific aims of this project can be introduced in two headlines;

- (i) To develop a 1-DOF mechanism to experimentally determine how much relative displacement, amplitude and frequency is required for active feedback with electrovibration method;
- (ii) To develop a 2-DOF planar mechanism to provide active feedback on a touch display actuated by electrovibration method;

Consequently, 2-DOF active feedback system is aimed to be obtained properly via our experimental procedure. The expected result of experiments is to feel directional force on touch screens when the finger is stationary in contrast to passive haptic system. In this thesis, active haptic feedback in two dimensions is achieved on a touch screen using electrovibration method which has not been implemented before in the literature.

2. LITERATURE REVIEW

Comparing touch screens with physical buttons of the electronic devices, the main difference is that touch screens are programmable and improvable tools. So far, touch screens of electronic devices provide only basic vibrations as haptic feedback. In the future, it is obvious that detailed and rich haptic feedback should be implemented on touch screens which will offer high level of satisfaction of touch sensations to users [13, 14]. According to the studies in the literature, users can feel a variety of textures [7], 3D objects [15] and their combinations [16] on tactile displays by modulating friction between the finger and the touch screen. This kind of studies in which tactile feedback is produced by changing the friction is called surface haptics. Below, the literature about this subject and the gaps in the state of art surface haptic devices are given.

The most common example of haptic technology for the current touchscreens is that users can be stimulated when their cell phones vibrate. These vibrations are obtained via an eccentric mass rotated by a small electric motor. Thanks to this simple design, the trembling on all devices through various frequencies attracts the attention of users [2]. One step further of this application, there are piezoelectric actuators mounted on the glass surface providing vibration. Thus, only the screen vibrates instead of the entire device that the more meaningful sense of touch can be created [17]. Today, it is the last point that touch screen applications has arrived so far in terms of haptic feedback.

Enriching the user experience with touchscreen is an important issue in recent years. The biggest obstacle of applying mechanical solutions for haptic feedback is to block the image on the screen [17, 18]. In recent years, tactile feedback systems by controlling the friction between the transparent touch pad and finger has been tested in various research laboratories [19, 20]. By altering the friction force acting between the fingertip moving laterally and the touchscreen, geometrical and material properties of the virtual object can be presented to the user. Robles-De-La-Torre and Hayward [21] showed how lateral forces affect the perception of geometric properties of objects. There

are two methods in the literature to change the surface friction which are ultrasonic vibration and electrovibration methods.

2.1. Ultrasonic Vibration Method

The common approach in ultrasonic vibration method is to use resonance of glass plate and vibrate the entire touch screen with complex waveforms to achieve sufficient amplitude in order to lift the skin [22] as seen in Figure 2.1. Vibrating surface with a very high frequency creates a squeeze film of air between finger and surface [19, 23]. This decreases amount of friction force [24] because surface friction coefficient is inversely proportional to the vibration amplitude [25]. For actuation, electromagnetic or piezoelectric devices are used in various studies. These actuators deliver vibratory signals while the contact take place between the touch screen and the user's skin. The range of modulation frequencies from 20 to 800 Hz have been reported as the most perceivable bandwidth by tactile perception [8, 26, 27].

Through the active touch, Robles-De-La-Torre and Hayward [21] showed how lateral force can overcome object geometry in the perception of shape. In an another study, a 3D feature is rendered on a touch surface by adjusting frictional force [15]. With this method, the virtual touch on various surfaces can be created [28].

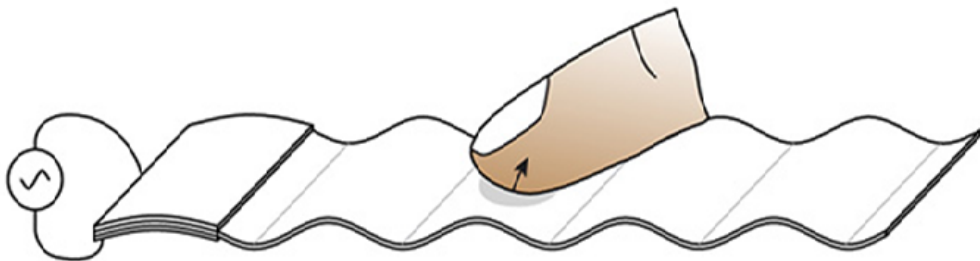


Figure 2.1. A touch surface is vibrated at its resonant frequency using a piezoelectric actuator in the ultrasonic vibration method. Reprinted from [22].

However, especially one of the significant disadvantage of the ultrasonic vibration method is that higher amount of energy is needed for the actuation compared to the electrovibration method. For this reason, the electrovibration method is more promising for practical applications [29]. Energy losses is a crucial factor for the ultrasonic vibration method in which Giraud *et al.* [30] argued that the major reason for energy inefficiency comes from the dielectric dissipation in the actuator. Even if this method is good at controlling friction force on a surface, it becomes difficult to modulate lateral forces in larger displays and the result is noisy [31]. These downsides limit application of ultrasonic vibrations in real life.

2.2. Electro vibration Method

The second method, electrovibration, is able to alter surface friction like the ultrasonic vibration method, but achieves it without using any mechanical actuation. Instead, the electrovibration method relies on creating electrostatic forces between finger and display [20, 32] which increases the normal and thus friction force [29, 32]. In fact, electrovibration alters surface roughness when the electrically insulated fingers are moving over a conductive surface (e.g. electrodes) where a periodic AC voltage applied to a conductive surface [33]. Alteration of roughness on a tactile display is created between the tactile display and the outer layer of the skin which is isolator when friction force is modulated by electrostatic force. So by controlling electrostatic force, friction force changes and as a result of this, surface properties change. This method is based on modulating lateral friction force between finger and display by varying amplitude and frequency of the electrostatic force [29]. The finger and touch screen illustration is seen in Figure 2.3.

Electrostatic force can be basically represented by the parallel-plate capacitor theory [34]–[35]. Two plates attract each other regarding the Coulomb’s law as long as a high voltage is applied to two parallel plates in which positive and negative charges go to boundry of each plate. Electrostatic force formula is given as:

$$F = \frac{\varepsilon AV^2}{2d^2} \quad (2.1)$$

where A is the area of the plate, d is the distance between the plates, ε is the permittivity of free space, and V is the applied voltage between plates.

Electrically induced vibrations were first found by Mallinckrodt *et al.* [33] while high voltage AC conductor with a thin insulator layer was being touched accidentally in 1953. This AC effect was later replaced with the name electrovibration and studied in more detail by Grimnes [36] who also tried both bare and insulating surfaces. Regarding to his studies, it was noted that the electrovibration intensity seemed to increase with the dryness of the skin. Current flowing in the skin were measured in the micro amper level, much below the traditional electro-cutaneous sensation limit of approximately 1 mA [36].

In haptics science, Strong and Troxel [34] first used electrostatic force for creating textures on a haptic display. Also, they first adapted the mathematical model of the parallel plate capacitor into the surface and finger interaction in electrovibration method by taking relative permittivity of the outer layer of the skin and dielectric layer into account. The outer layer of the skin is also called stratum corneum as seen in Figure 2.2, which consists of mostly dead cells having almost 200 micron thickness at the fingertip [37]. Accordingly, the equation is given below:

$$F = \frac{\varepsilon_o AV_t^2}{2\left(\frac{d_d}{\varepsilon_d} + \frac{d_s}{\varepsilon_s}\right)^2} \quad (2.2)$$

where F represents the electrostatic force on the skin, A is the contact area, ε_0 is the permittivity of free space, V_t is the total applied voltage between the ground and the surface, d_s is the thickness of the stratum corneum of skin, d_d is the thickness of the

dielectric insulating layer, ε_s is the relative permittivity of the skin and ε_d is the relative permittivity of the dielectric layers in this mathematic model.

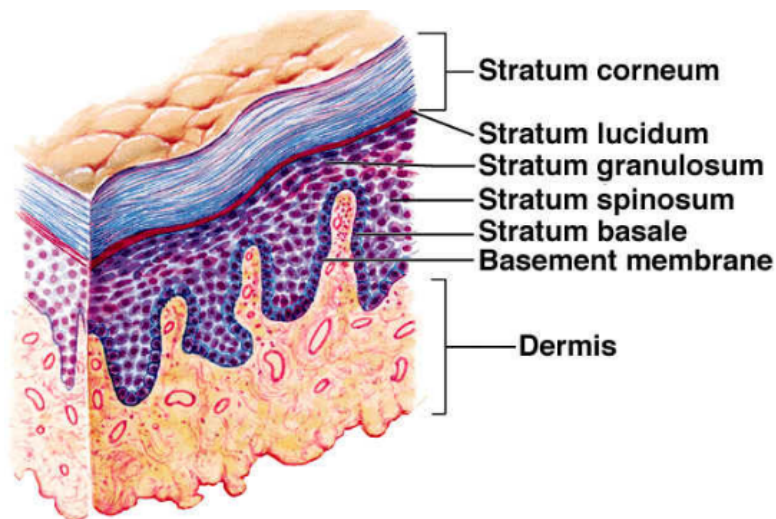


Figure 2.2. Layers of skin tissue. Reprinted from [22].

To create high friction on a surface using electrostatic force, Beebe *et al.* [38] developed a polyimide-on-silicon tactile display with 100 Hz pulses. Later on, Vezzoli *et al.* [39] introduced an electrostatic force model regarding the frequency dependent electrical parameters of conductive layer of human skin. Using this model, the transfer function of voltage through stratum corneum was calculated. Theoretical and experimental results coincided well with each other.

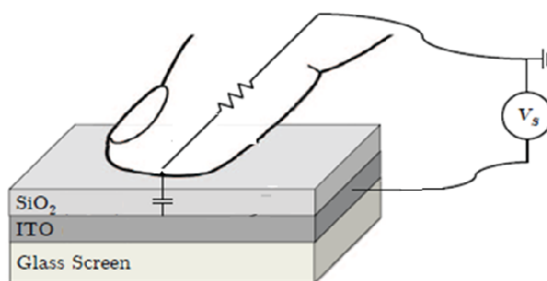


Figure 2.3. The layers of the electrostatic tactile display. Reprinted from [29].

While the electrovibration method is based on AC current, the electroadhesion method introduced by Johnsen-Rahbek is based on DC current. The electroadhesion

term was first used in 1923 by Danish scientists Alfred Johnsen and Knud Rahbek [40]. When they were working with polished lithographic stone and metal surfaces, high DC voltage was applied between polished stone and metallic plate touching each other. Since, as a result of the experiment, the remarkable adhesion was accomplished, the name electroadhesion was first used to describe this physical phenomenon. Lastly in 2015, the great progress has been taken with DC electroadhesion method by Shultz *et al.* [41] who has created considerable amount of friction force by using an electrostatic chucking device greater than previously reported in literature. Also, his study which has not been implemented yet to touch screens is encouraging for the future since remarkably high normal forces can attract the bare fingertip using only milliwatts of electrical power.

Researchers have used human detection threshold to study the electrostatic effect further. Agarwal *et al.* [35] observed the relationship between dielectric thickness and voltage at the detection threshold, and Kaczmarek *et al.* [42] investigated the differences in detection for positive and negative voltages. While these efforts have studied human response to electrical stimulations, none have measured the mechanical effect of electrostatic attraction, and a detailed understanding of the finger-surface interface is still lacking which will be explained as much as possible in the subsection Tribology of the Fingertip.

Although the friction modulation creates different feelings of texture [43, 44, 45], there are a few fundamental problems with this method. First, the direction of lateral force is not controlled and is always against the motion of the finger. The second weakness of electrovibration is that only a moving finger receives a feedback. In other words, a finger does not get any feedback in stationary form. For this reason, finger must move on a passive system. Contrary to a passive system, finger can receive directional tactile feedback if the touchscreen is moved relative to finger, which is called active feedback. Without active feedback, a virtual button cannot be pressed and common interaction in virtual environment is not possible.

Rest of the problems of electrovibration method is related with electrical properties of human skin which is still investigated, even though many studies have been done on this method so far [33, 34]. Being electrically grounded changes the power of electrostatic attraction effect. Also, a further procedure of electrovibration method has not been preferred since current flow is not favorable for finger and it might results in weaker touch sensation due to having different electrical impedance of human skin. Recently, towards to this problem Kim *et al.* [46] has proposed current controlled electrovibration method to avoid non-uniformity of sensation regardless electrical grounding. In this study, it is claimed that current feedback method provides higher uniform intensity of effect than the conventional voltage control method.

2.3. Tribology of Fingertip

The tribology of the fingertip has been examined by several researchers, particularly in the field of fingertip and contacting surface interaction. Even though the mechanical properties of human skin varies substantially from person to person, the fingertip has been mostly considered as a viscoelastic material. Tomlinson *et al.* [47] used a simple device under sliding motion of fingertip on a surface to determine a relationship between normal force and lateral friction force. A linear relationship is found between friction force and normal force as the fingertip arrives its compressibility limit. The two major mechanisms taking place regarding friction on viscoelastic materials are adhesion and hysteresis [48], which are also valid for the skin. In the adhesion mechanism, local bonds occur at the higher loads leading the friction forces. For the relatively lower loads, the linear relationship between normal force and lateral friction force is not valid because of the hysteresis as seen in figure 2.4. Furthermore, increasing the sliding speed increases the friction coefficient of viscoelastic materials. For example, the friction coefficient of rubber increases at higher speeds because of the increasing surface temperature causing an increase in contact area [49]. Several studies also showed that the friction coefficient increases if the hydration occurs on the skin surface since the liquid bridging between fingertip and surface brings higher friction owing to the shear forces set up [50, 51]. The dynamic friction coefficient has been

investigated in variety of the studies, except a few examined static friction due to the complication arising from velocity dependence of viscoelastic materials [52]. The other difficulty is the discrepancy of static and dynamic behaviour of viscoelastic materials which is not seen with non-viscoelastic materials. However, Lewis *et al.* [53] and Koudine *et al.* [54] measured the static friction coefficient of fingers, and found this to be greater than the kinetic friction coefficient.

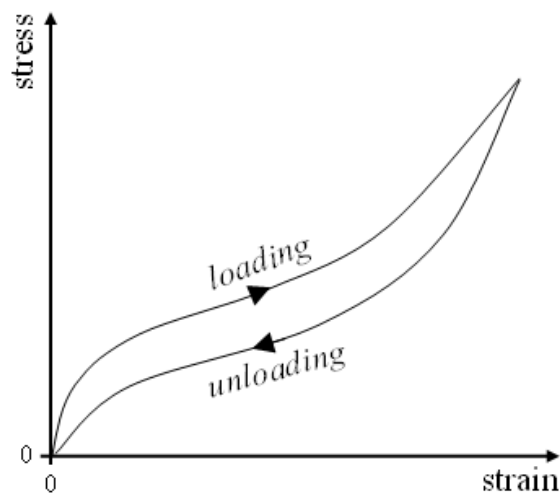


Figure 2.4. The hysteresis loop of viscoelastic materials represents the energy dissipation during load-unload cycle.

3. METHODOLOGY

To improve haptic feedback on touch screens, 2-DOF active feedback is aimed to be created using electrovibration method. In order to achieve 2-DOF active feedback, the experimental methods are defined and introduced in two stages. In the first stage, the directional force is investigated leading an active feedback. Parameters such as relative displacement, amplitude and frequency of the excitation signal affecting the feasibility of active feedback are determined. In the second stage, a 2-DOF mechanism is developed to provide 2-DOF active feedback on a tactile display using electrovibration method.

To be able to create directional force acting to a stationary finger from an electrostatic tactile display, the following steps should be realized: (1) a relative motion between the finger and the display must be achieved, (2) adequate electrostatic attraction must be guaranteed with a high-voltage periodic excitation, and (3) electrostatic force must be synchronized with the motion of the display. For this purpose, electrostatic attraction is periodically enabled and disabled as the touch screen goes back and forth. An example of the input signal for the electrostatic display is given in Figure 3.1. Assuming that a display has a sinusoidal movement with respect to finger, applying periodic high-voltage excitation, such as a square wave, in forward or reverse motion of the display leads to a directional force. In order to demonstrate whether directional force can be achieved by an electrostatic tactile display, we have developed a 1-DOF mechanism and conducted a number of experiments. Measurements were taken with the subject's fingertip covered with an antistatic finger cot.

In order to change the direction of the force acting to the finger in two dimensions on the tactile display, the following steps should be realized: (1) Same steps for creating directional force must be achieved and (2) the motion of the tactile display in X and Y axes must be synchronized with the electrostatic force. For this purpose, electrostatic attraction is periodically enabled and disabled as the touch screen goes back and forth in X and Y axes. The sinusoidal movement of the tactile display is obtained through

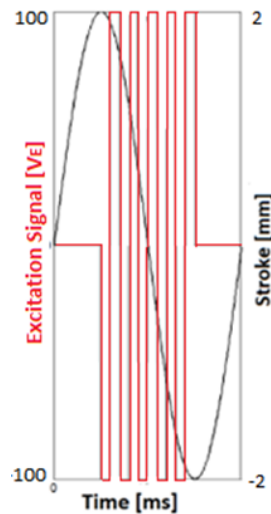


Figure 3.1. Input signals to create active feedback on an electrostatic tactile display. Periodic square wave excitation for electrostatic attraction is synchronized with the sinusoidal motion of the display.

two centric slider crank mechanisms. To show whether directional force can be oriented at different angles on the electrostatic tactile display, the 2-DOF mechanism is used to conduct a number of experiments. Measurements are collected by a force sensor using an artificial fingertip. In the next subsections, both one dimensional and two dimensional experimental setups are introduced, and the experiments are described.

3.1. Experimental Setups

3.1.1. 1-DOF Experimental Setup

The experimental setup to investigate active tactile feedback consists of a 50 mm \times 100 mm capacitive touch screen, a shaker (Bruel and Kjaer 4809), a force sensor (ATI Nano 17) and a support for the hand to stabilize the index finger on top of the touch screen as shown in Figure 3.2. The screen is attached to a linear guide (model MR 7, PBC) and moved back and forth by the shaker. The force sensor is attached to the left index finger of the subject from the side using a strong double-sided tape. Together with the support, this can hold the finger firmly during the experiments. Thus, the

finger is stationary throughout the experiments and the normal contact forces were approximately 0.1 N. Also note that, the subject put on an antistatic finger cot.

The control schematic and block diagram for the experimental setup are shown in Figures 3.3 and 3.4, respectively. Both excitation signals (V_E and V_S , inputs for the capacitive touch screen and the shaker respectively) are modeled and synchronized in NI Labview. The signals are converted into analog voltages using a data acquisition card (NI USB-6218) and two amplifiers (TREK PZD 700 A and LEPY LP-2020A) are used to drive the touch screen and the shaker, respectively. The sampling rate in measurements and the update rate for excitation signals are 1 kHz.

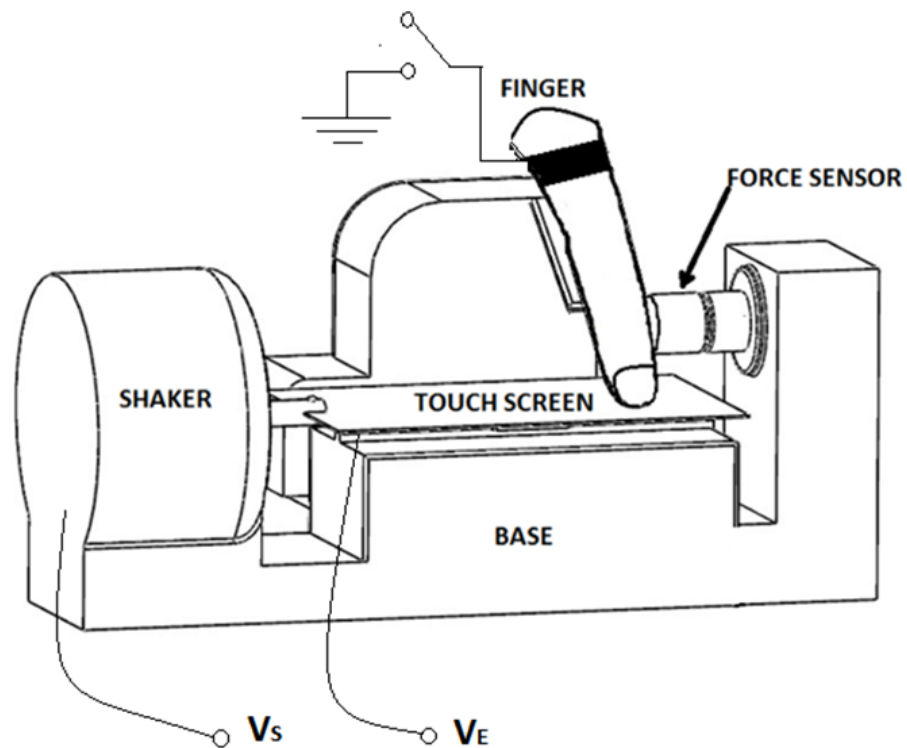


Figure 3.2. Illustration of the experimental setup used to measure lateral forces acting on the index finger.

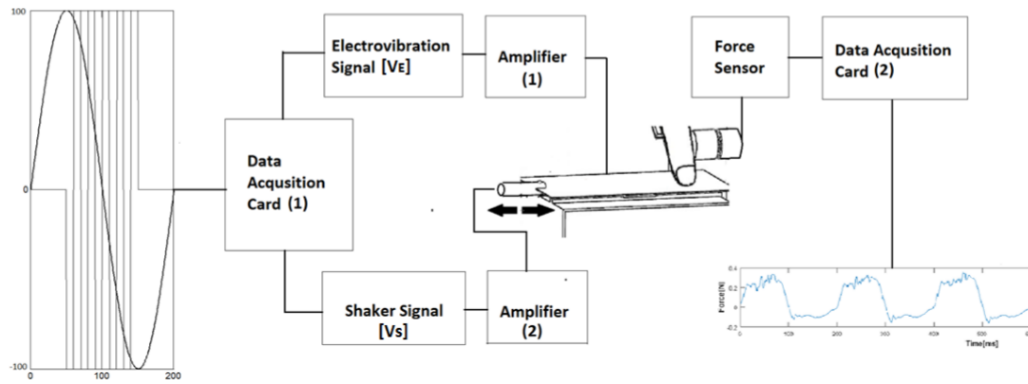


Figure 3.3. Control schematic of the 1-DOF experimental setup.

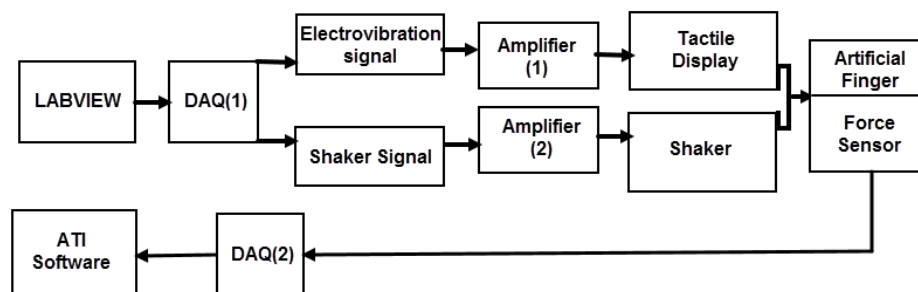


Figure 3.4. Block diagram of the 1-DOF experimental setup.

3.1.2. 2-DOF Experimental Setup

In the second part of the study, a two dimensional experimental setup has been developed to investigate 2-DOF active tactile feedback. 3D render of the setup is seen in Figure 3.5.

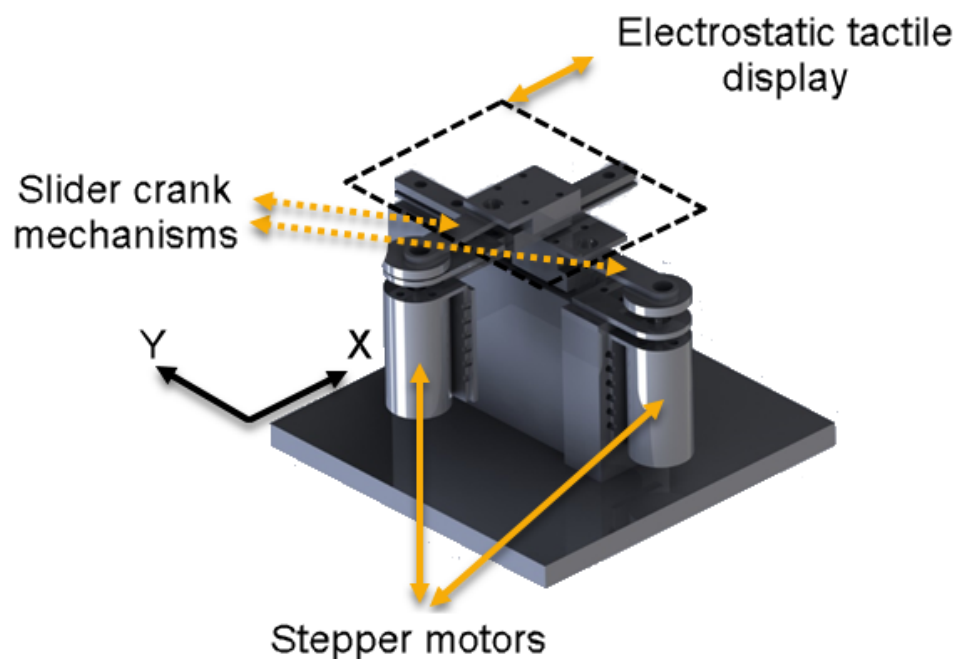


Figure 3.5. 3D render of the 2-DOF mechanism which consists of two stepper motors, two slider crank mechanisms, a touch screen and a base.

The 2-DOF experimental setup consists of a 50 mm × 100 mm capacitive touch-screen, two independent slider crank mechanisms actuated by step motors having a 1.8 degree step angle (POLOLU, Nema-14), micro controller (Arduino Uno), an artificial finger and a force sensor (ATI Nano-17). The screen is attached to linear guides (model MR7, PBC) and moved in 2D by the slider crank mechanisms as seen in figure 3.6.

The control schematic and block diagram for the 2D experimental setup are shown in Figures 3.7 and 3.8. The excitation signals are modeled and synchronized in NI LABVIEW and Arduino Uno, micro controller, which enables to actuate step

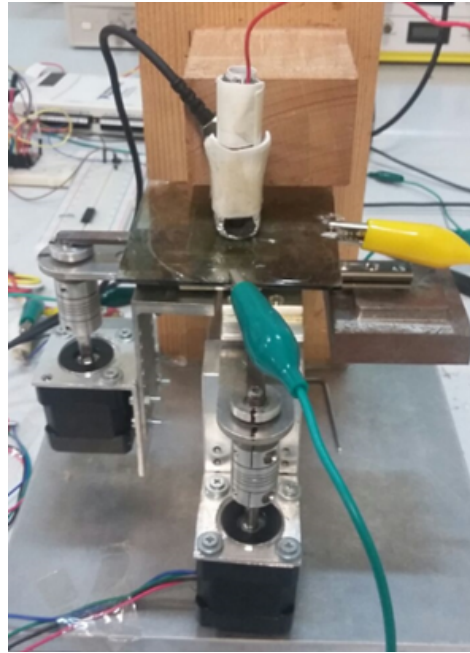


Figure 3.6. The experimental setup for 2D measurements.

motors using A4988 motor driver carrier. The input signal of tactile display, V_E , is built in excel and embedded into the box shown in figure 3.7, the input signal of step motor driver circuit, V_S , is built by using simulate DC signal tool in NI LABVIEW. Since both micro controller code and NI LABVIEW control panel works independently, the Arduino code loop is programmed to be triggered by analog signal coming from the NI LABVIEW program to be synchronized with the excitation signal of electrostatic tactile display. Also, 20 ms delay has been added to excitation signal of tactile display due to the latency of arduino output signal actuating the step motors. The signals are converted into analog voltages using a data acquisition card (NI USB-6218). While an amplifier (SVR 150/3 Piezomechanik GmbH) is used to amplify the excitation signal of the touch screen, the DC power supply (Agilent U8032A) is used to drive the stepper motors. The sampling rate in measurements and the update rate for excitation signals were 10 kHz.

3.1.2.1. Centric slider crank mechanism. Two slider crank mechanisms were developed for 2D experimental setup to drive the touch screen in X-Y plane due to the

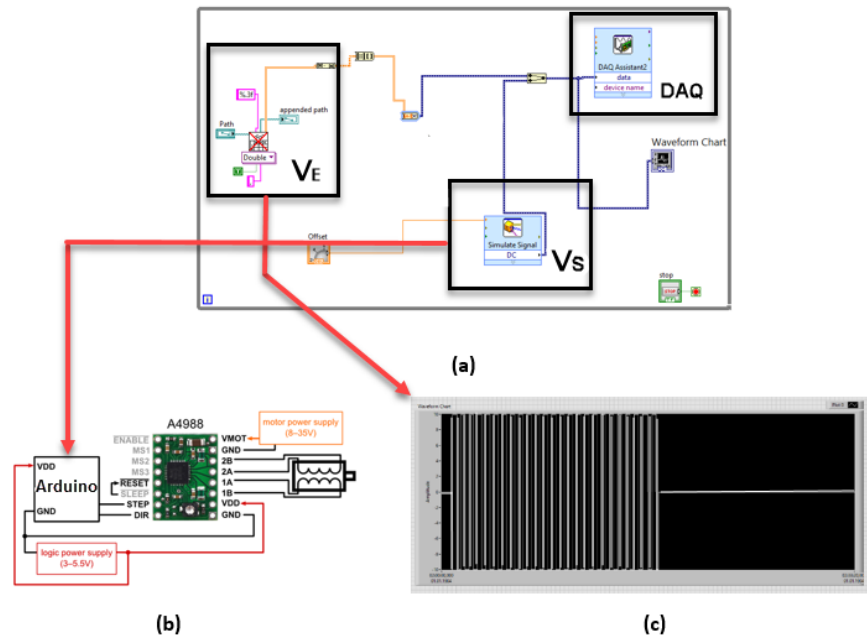


Figure 3.7. Control schematic. a) Labview control panel with control blocks, b) stepper motor driver circuit, and c) square wave excitation signal with 20 ms delay.

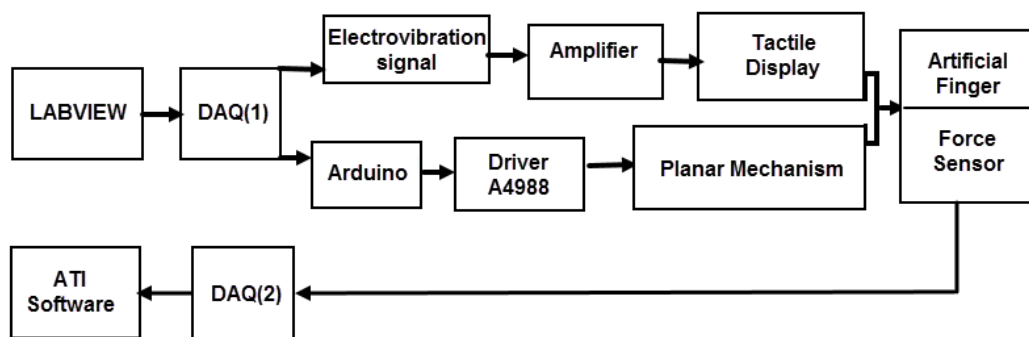


Figure 3.8. Block diagram of the 2-DOF experimental setup.

fact that it is easy to generate such oscillatory motion. Slider crank mechanism has variety of applications, which is employed to transform the rotary motion to rectilinear translational (sliding) motion or vice versa [55]. Particularly in our system, the centric slider crank mechanisms which is shown in Figure 3.9 establish connection between the step motors and the touch screen to convey back and forth strokes with the same timings unlike to the offset slider-crank mechanisms. Since the finger is stationary, crank length directly corresponds half of the relative displacement between the finger and the touch screen. In order to obtain 4 mm displacement of the tactile display (x) the crank length (r) was selected as 2 mm. The coupler length (l) was selected as 50 mm in order to obtain smaller ϕ which leads lower torque applied to crank shaft.

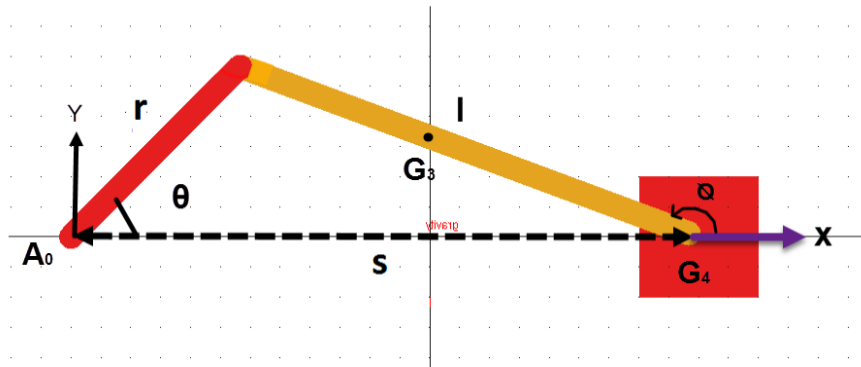


Figure 3.9. Centric slider crank mechanism modeled in ADAMS.

In order to move the touch screen in each axes independently, two slider crank mechanisms were required. For this reason, the one which excites the tactile display in Y axis, must also carry the second slider crank mechanism. Therefore, the setup was designed as light as possible to decrease the torque requirement of the stepper motor which actuates the tactile display in Y axis. Stepper motors were preferred instead of DC motors due to their position control characteristics which is more suited for our experiments. In order to select proper stepper motors, torque about crank shaft were calculated only for the slider crank mechanism working along Y axis by using kinematic Equations (3.1)–(3.12) and dynamic Equations (3.13)–(3.20) via MATLAB. The free

body diagram of centric slider crank mechanism which works along Y axis is shown in Figure 3.10. Also, this slider crank mechanism is simulated in ADAMS as shown in Figure 3.9. The crank shaft and coupler link are assumed as rigid bodies due to the negligible axial elongation, and friction force is not ignored on the linear guides. Trigonometric method is used for kinematic analysis in coordinate system [56]. Joint clearances at the crank-pin and slider-pin center were ignored in kinematic calculations.

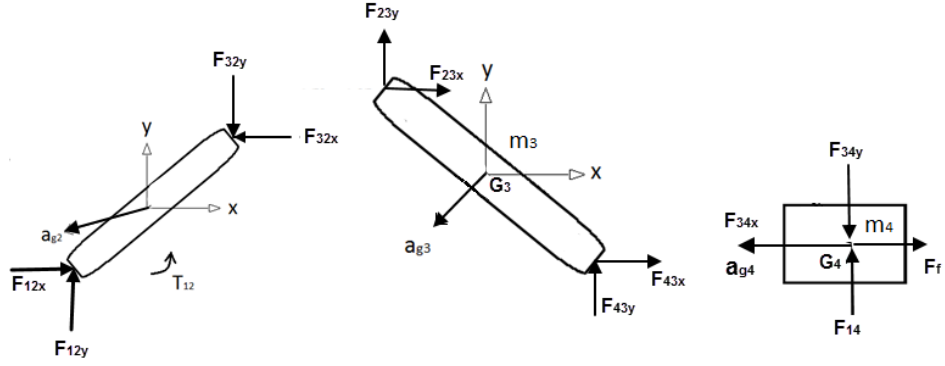


Figure 3.10. Free body diagrams of the centric slider crank mechanism. Mass of the coupler link, m_3 , is 0.03 kg, and its center of gravity is in the middle. The mass, m_4 which is 0.8 kg, corresponds to the total mass of the tactile display and the slider crank mechanism working along X axis. To calculate the friction force, F_f , the dynamic friction coefficient is 0.25 based on the data sheet.

In order to derive the kinematic equations, loop-closure equation is written as below:

$$re^{i\theta} = s + le^{i\phi} \quad (3.1)$$

From equation 3.1, ϕ and s are derived as:

$$\phi = a \sin\left(\frac{r}{l} \sin\theta\right) \quad (3.2)$$

$$s = r \cos\theta - l \cos\phi \quad (3.3)$$

In order to calculate the acceleration values, the position and velocity equations of the center of gravity of coupler link and m_4 must be written and differentiated as below:

$$\dot{\phi} = \frac{r}{l} \omega \frac{\cos\theta}{\cos\phi} \quad (3.4)$$

$$\ddot{s} = r\omega \frac{\dot{\phi}\cos\theta\sin\phi - \omega\cos\phi\cos(\phi - \theta)}{\cos^2\phi} \quad (3.5)$$

$$\ddot{\phi} = \frac{r}{l} \frac{\dot{\phi}\cos\theta - \omega\cos\phi\cos\theta}{\cos^2\phi} \quad (3.6)$$

$$A_0G_3 = A_0G_4 + G_4G_3 = s + \frac{l}{2}e^{i\phi} \quad (3.7)$$

$$\nu_{G3} = \dot{s} + i\frac{l}{2}\dot{\phi}e^{i\phi} \quad (3.8)$$

$$a_{G3} = \ddot{s} + i\frac{l}{2}\ddot{\phi}e^{i\phi} - \frac{l}{2}\dot{\phi}^2e^{i\phi} \quad (3.9)$$

$$a_{G3x} = \ddot{s} - \frac{l}{2}(\ddot{\phi}\sin\phi - \dot{\phi}^2\cos\phi) \quad (3.10)$$

$$a_{G3y} = \frac{l}{2}(\ddot{\phi}\cos\phi - \dot{\phi}^2\sin\phi) \quad (3.11)$$

$$a_{G4x} = \ddot{s} \quad (3.12)$$

Following the kinematic equations, the kinetic equations can be written by using the free body diagram as below. Considering the sliding mass, m_4 :

$$F_{34x} = m_4 a_{G4x} + \text{sign}(\dot{s}) \mu m_4 g \quad (3.13)$$

$$F_{34y} = F_{14} \quad (3.14)$$

Considering the coupler link:

$$F_{23x} + F_{43x} = -m_3 a_{G3x} \quad (3.15)$$

$$F_{23y} + F_{43y} = -m_3 a_{G3y} \quad (3.16)$$

$$I\ddot{\phi} = F_{43y} l \cos\phi + F_{43x} l \sin\phi \quad (3.17)$$

Since the mass of crank is too small, the inertial effects of crank can be neglected, and the static equation of the crank is written as below:

$$F_{12x} = F_{32x} \quad (3.18)$$

$$F_{12y} = F_{32y} \quad (3.19)$$

Through the kinetic equations, torque about crank shaft, T_{12} , is found as below:

$$T_{12} = -F_{32x} r \sin\theta + F_{32y} r \cos\theta \quad (3.20)$$

Velocity and acceleration profiles of the tactile display were plotted from ADAMS as seen in Figure 3.11. When the tactile display is driven at 5 Hz, maximum linear velocity is 65 mm/s at 90 and 270 degree angle while maximum acceleration is 1900 mm/s² at 0 and 180 degree angles.

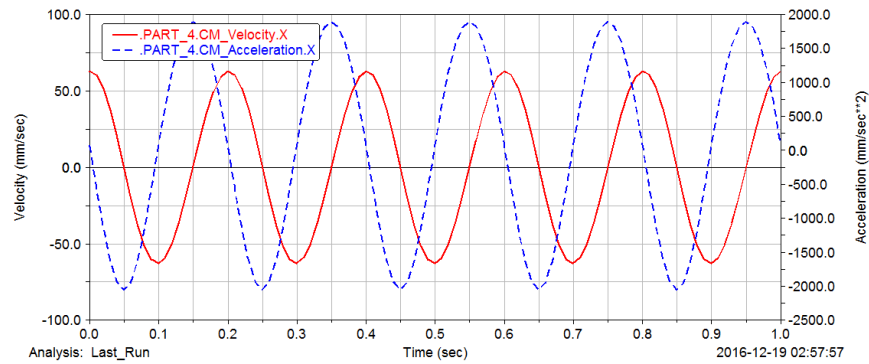


Figure 3.11. Velocity and acceleration profiles of the tactile display along X axis.

Torque analyses were run at 1 Hz, 5 Hz, 10 Hz, 25 Hz and 50 Hz of constant oscillations of the tactile display in order to define total torque requirement for higher relative velocities between the finger and tactile display which are seen Table 3.1. The results of the torque analyses from ADAMS are plotted as absolute values which are shown in Figures 3.12, 3.14, 3.16, 3.18 and 3.19. According to the torque analyses, the peak values of total torque about crank shaft 8 Nmm at frequency of 1 Hz, 8.4 Nmm at frequency of 5 Hz, 12.5 Nmm at frequency of 10 Hz, 46 Nmm at frequency of 25 Hz and 167 Nmm at frequency of 50 Hz. These values are required for the stepper motors to actuate the tactile display. The peak total torque values occur at 46, 133, 223 and 316 degree angles. On the other hand, the maximum holding torque of the step motor (Nema 14) at frequency of 1 Hz, 5 Hz, 10 Hz, 25 Hz and 50 Hz are around 130 Nmm, 120 Nmm, 65 Nmm, 20 Nmm and below 1 Nmm, respectively, as shown in Figure 3.20. Regarding the required total torque values to actuate the system, the frequency of 25 Hz exceeds the holding torque limit of the stepper motor. Consequently, the frequency of motion could be 10 Hz, but considering the extra load of fingertip, the frequency of motion is kept at 5 Hz. Additionally, higher models of this stepper motor can not supply enough holding torque beyond 15-20 Hz, and higher weight and size increase the torque requirement for the second actuator.

Table 3.1. Maximum torque values [Nmm].

Speed	ADAMS	MATLAB	MATLAB (without friction)
1 Hz	8	7.6	0.1
5 Hz	8.4	8	2
10 Hz	12.5	12	6.5
25 Hz	46	-	-
50 Hz	167	-	-

Moreover, the calculated total torque about the crank shaft to actuate the system increases exponentially as the speed of motor shaft increases due to either the increasing inertial forces or the friction forces on linear guides. So as to justify how inertial forces and frictional forces effect the torque results, torque analyses are done in MATLAB as seen in Figures 3.13, 3.15 and 3.17. Based on the results, frictional forces are the major factor affecting the total torque values until the 10 Hz. On the other hand, even though, the inertial forces have quite low effect on total torque values at 1 Hz and 5 Hz, the inertial forces increase the torque values exponentially ahead of 10 Hz.

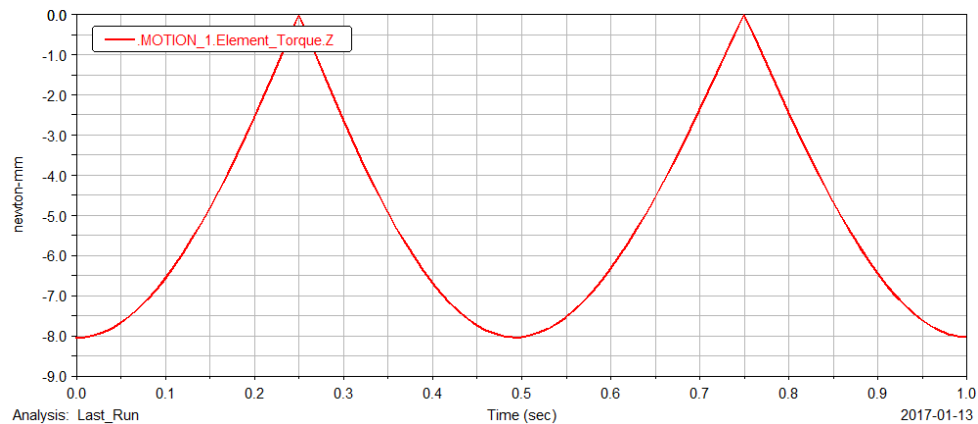


Figure 3.12. Torque about crank shaft at 1 Hz of frequency.

Fast fourier transform was applied to the resultant torque at frequency of 5 Hz as seen in Figure 3.21. According to the results, 10 Hz and its complex harmonics are occurred until 50 Hz with 10 Hz increments.

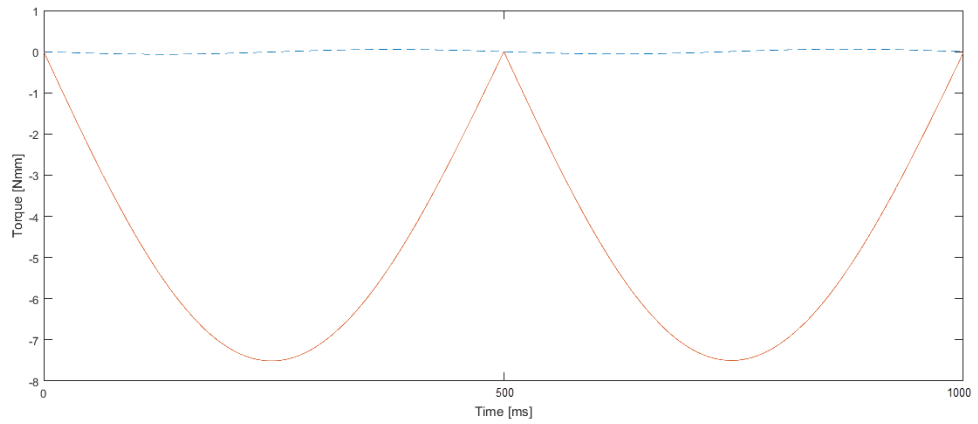


Figure 3.13. The calculated torque about crank shaft at 1 Hz of frequency in MATLAB. The dashed line shows the torque value without friction force on the linear guides.

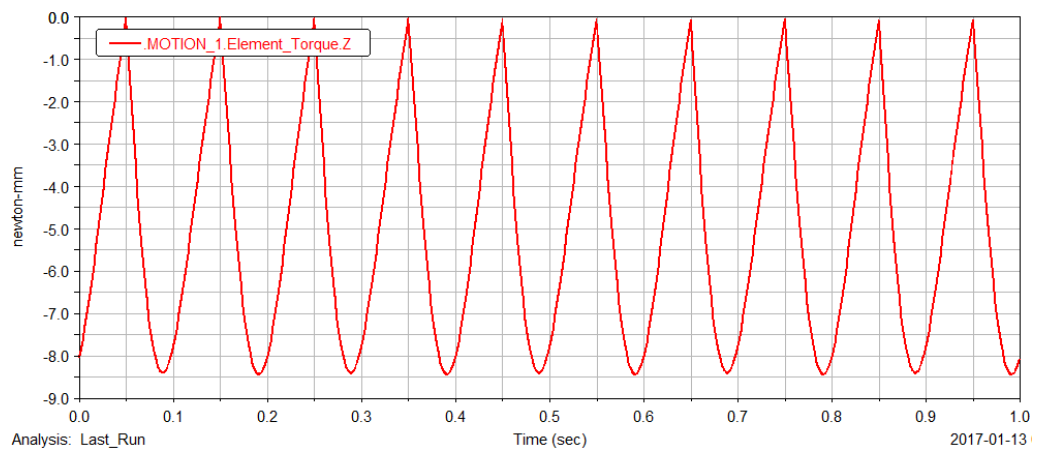


Figure 3.14. Torque about crank shaft at 5 Hz of frequency.

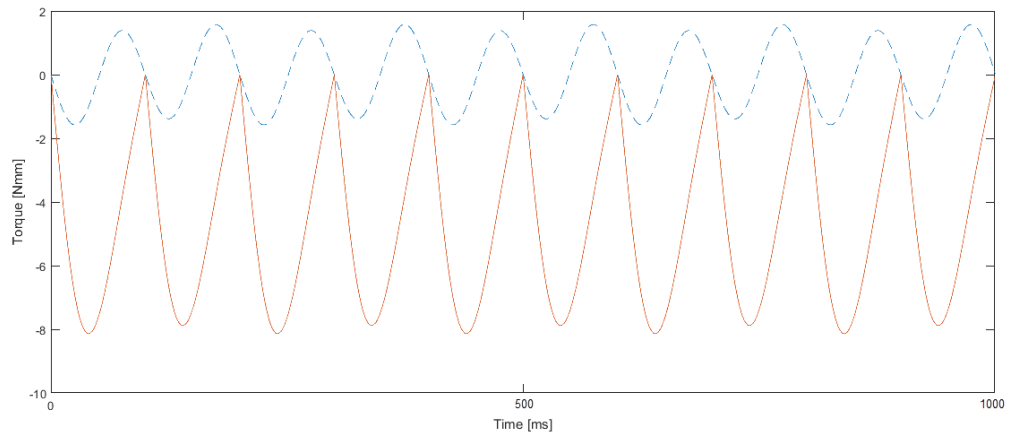


Figure 3.15. The calculated torque about crank shaft at 5 Hz of frequency in MATLAB. The dashed line shows the torque value without friction force on the linear guides.

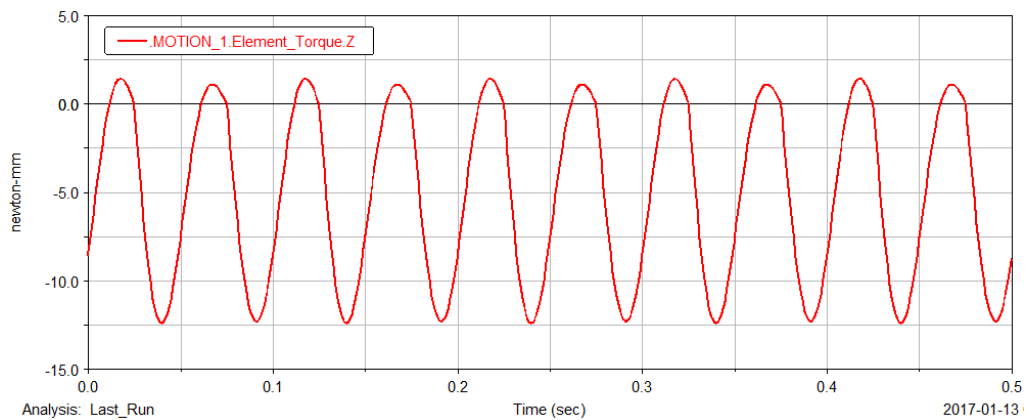


Figure 3.16. Torque about crank shaft at 10 Hz of frequency.

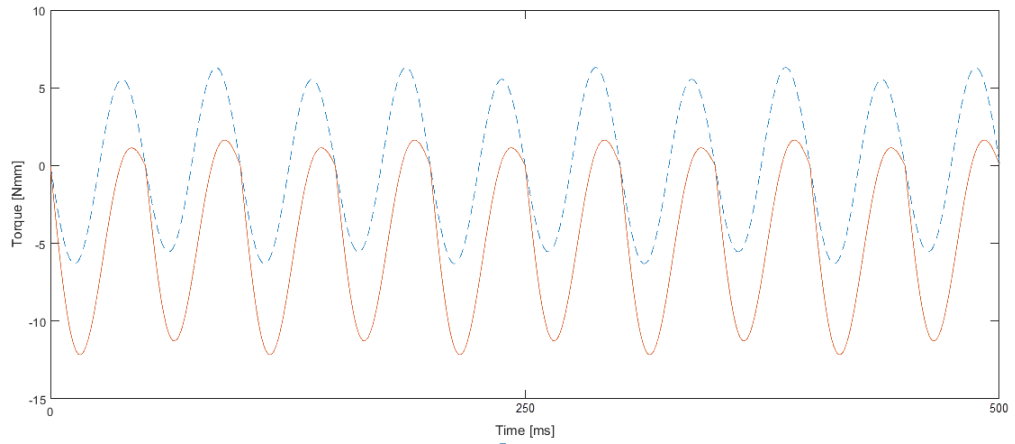


Figure 3.17. The calculated torque about crank shaft at 10 Hz of frequency in MATLAB. The dashed line shows the torque value without friction force on the linear guides.

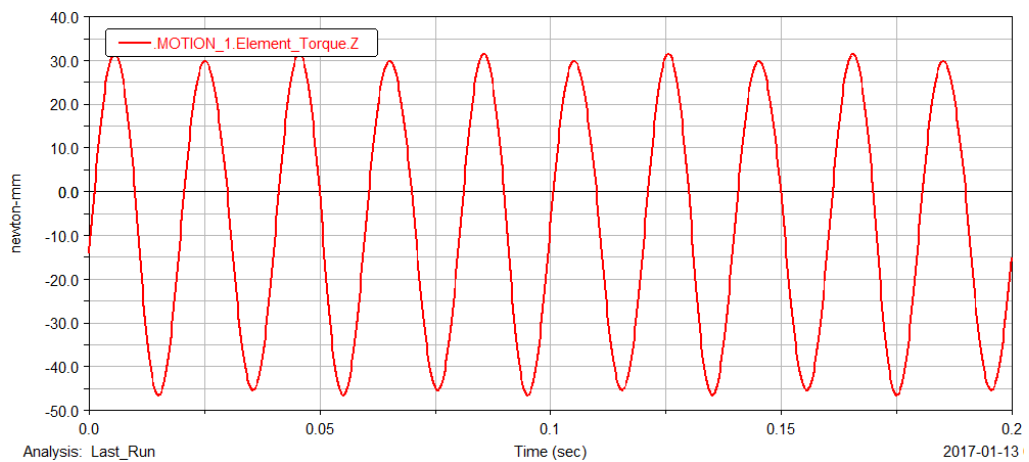


Figure 3.18. Torque about crank shaft at 25 Hz of frequency.

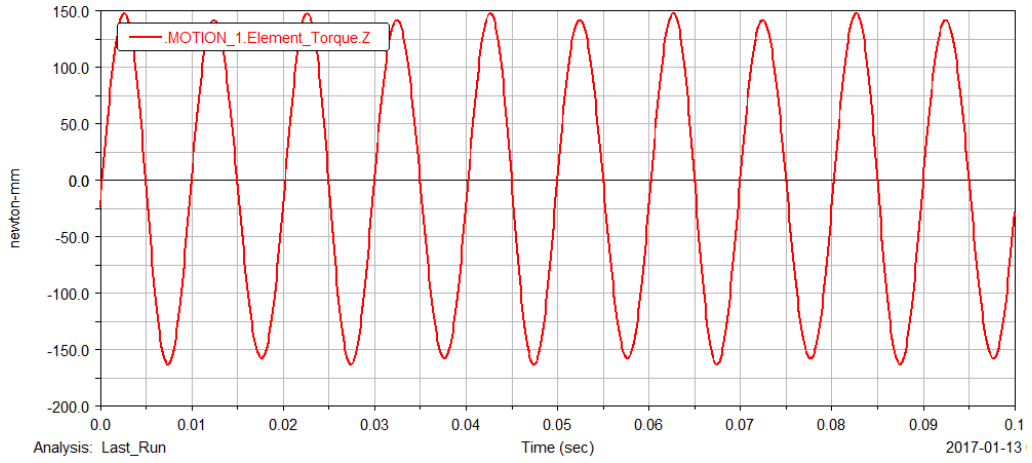


Figure 3.19. Torque about crank shaft at 50 Hz of frequency.

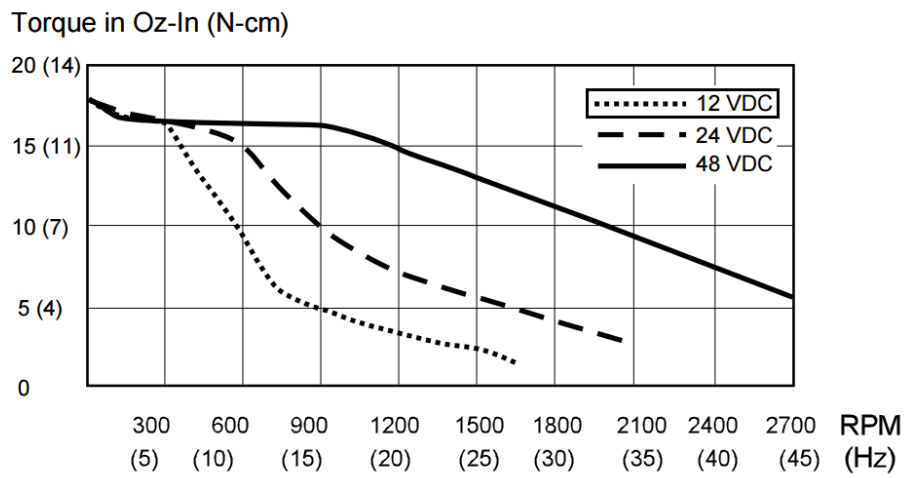


Figure 3.20. Torque-speed curve of the stepper motor (POLOLU, Nema 14) which was driven at 12 VDC.

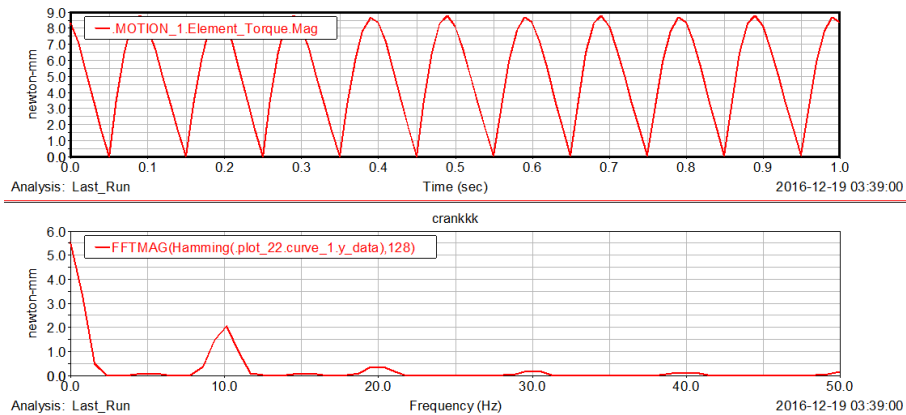


Figure 3.21. FFT is applied to torque values about crank shaft at frequency of 5 Hz. Harmonics of the input are seen at 10 Hz increments.

Additionally, the current values drawn by the step motors were measured during the experiments to have an opinion about torque behavior of the step motors. Measurements were done under constant voltage, 12 VDC. 444 mA, 1009 mA and 1072 mA are read constantly for 5 Hz, 2.5 Hz and 1 Hz, respectively. As the speed increases under constant voltage, the current value exponentially decreases. In other words, supplied torque value decreases proportionally with respect to current values, as expected considering the torque speed curve. As a result, the two constraints which are the decreasing torque output of the stepper motor and increasing inertial forces of masses at higher speeds restrict to drive the tactile display at higher frequencies.

3.1.2.2. Artificial finger. In the first experimental setup, the human skin was deliberately used to test the sensation of active feedback. In the literature, it was shown that electrostatic forces might be felt differently by different users due to the variable mechanical and electrical properties of skin [12]. In the second set of experiments, artificial finger was preferred in order to be protected from high voltage exposure. An artificial finger was made to be similar in size of a real finger tip as seen in Figure 3.22.

The artificial finger is composed of two layers where a rod covered with foam rubber and an aluminum foil which is conductive surface at the outer layer. In order

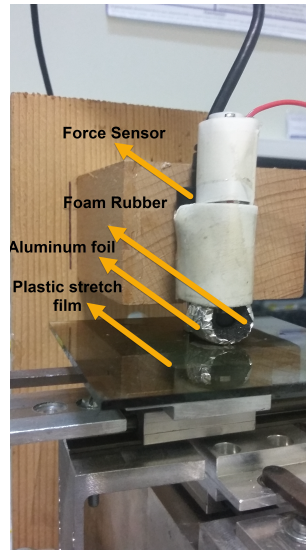


Figure 3.22. Components of the artificial finger. The force sensor is attached to the artificial finger using strong double-sided tape.

to represent the stratum corneum layer of the skin, a plastic stretch film is covered on the touch screen. Aluminum sheet corresponds the conductive layer of the skin. The foam rubber is also selected for representing the viscoelastic property of the finger tip. Besides, the friction coefficient between the aluminum sheet and plastic stretch film is around 0.30 while this coefficient between a skin and a glass surface is around 1.25 [57, 58]. The layers are mechanically and electrically compliant and having a flat contacting area in which the contacting area, 15 mm^2 is kept same as the contacting fingertip area in 1D experiments. Electrical and mechanical properties of the artificial finger and a real finger are summarized in Table 3.2.

Table 3.2. Electrical conductivity and elastic modulus of a bare finger and an artificial finger [59, 60, 61].

	Dielec. const. [@1GHz]	Elastic modulus [MPa]
Skin	4 - 6	0.023 (hydrated) - 0.3 (dehydrated)
Stretch film	2.4 - 2.6	-
Foam rubber	-	0.3 - 1

3.2. Experimental Procedures

3.2.1. 1D Measurements

Periodic high-voltage square wave signals (V_E) were fed into the capacitive touchscreen to create electrostatic attraction on the surface. The maximum peak-to-peak amplitude of the input signal was $397 V_{pp}$. The first natural frequency of the touchscreen was estimated around 110 Hz using Abaqus FEA software package. Exciting the screen at this frequency led to an undesirable and uncontrolled directional force acting to the stationary finger on the surface. In order to be away from this frequency and guarantee finger contact with the display, the tactile display was driven with an input signal (V_S) at 5 Hz at all three experiments. During the experiments, the normal contact forces were approximately 0.1 N.

Three experiments were conducted to examine the feasibility of active feedback on the electrostatic tactile display. Three parameters were investigated in these experiments: (1) amount of relative displacement between the finger and the touchscreen, (2) frequency of excitation signal for electrostatic attraction, and (3) amplitude of excitation signal for electrostatic attraction.

In order to conclude that a directional force can be generated which was investigated in the first set of experiments, two conditions must have been satisfied: 1) increased lateral force due to electrostatic attraction must be observed only in one-half of the periodic movement, and 2) lateral force must be equal to surface friction in the other half of the movement.

3.2.1.1. Relative displacement. The shaker was driven with sinusoidal input signals with three different amplitudes to find the minimum displacement necessary for active force feedback. The touchscreen was excited with 1, 2 and 4 mm strokes by varying the amplitude of the input voltage to the shaker. Since the finger was stationary, these values corresponded to the relative displacements between the finger and the

touchscreen. A ruler was attached to the base, and a point on the touch display was tracked to measure displacements. The motion of the shaker and the display were recorded by a camera and observed for calibration. The excitation signal to create electrostatic attraction was 270 Hz and $397 V_{pp}$ square wave which was periodically enabled and disabled as the touch screen went back and forth at 5 Hz. The finger was not electrically grounded in this experiment.

3.2.1.2. Frequency of electrostatic excitation signal. The tactile display was moved with 4 mm stroke, and the frequency of excitation signal for the electrostatic attraction was varied between 80 Hz, 120 Hz, 180 Hz and 270 Hz. Input signals for the tactile display and the shaker were synchronized as shown in Figure 3.1. The amplitude of the signal was kept constant at $397 V_{pp}$, and the finger was not electrically grounded. As a reference, the same experiment was performed while the electrostatic attraction is disabled.

3.2.1.3. Amplitude of electrostatic excitation signal. The amplitude of the 270 Hz excitation signal for the electrostatic attraction was reduced to $215 V_{pp}$. The relative displacements between finger and the touchscreen were 4 mm. As in the previous experiments, the excitation signal to create electrostatic attraction was periodically enabled and disabled at 5 Hz. Note that measurements were taken twice for $215 V_{pp}$: once for the electrically grounded finger and once for not. Grounding was performed to increase the electrostatic force.

3.2.2. 2D Measurements

As in the previous section 3.2.1, the tactile display was driven with an input signal (V_S) at 5 Hz. Periodic high-voltage square wave signals (V_E) were fed into the capacitive touchscreen to create electrostatic attraction on the surface. The excitation signal to create electrostatic attraction was 250 Hz and $397 V_{pp}$ square wave which was periodically enabled and disabled as the touch screen goes back and forth at 5 Hz. During the experiments, the artificial finger was attached to the force sensor which

was held firmly by using a strong double-sided tape. Thus, the artificial finger was stationary during the experiments and the normal contact forces are approximately 0.1 N.

Two experiments were conducted to examine the feasibility of 2-DOF active feedback on the electrostatic tactile display. Two conditions were investigated in these experiments: (1) 4 mm strokes in X and Y axes and 4 and 2 mm strokes in X and Y axes, and (2) Continuously rotating directional force.

If two conditions introduced in section 3.2.1 are satisfied, we can claim that directional force is oriented on the electrostatic tactile display, 2-DOF active feedback, which is analyzed in the second set of experiments.

3.2.2.1. Directional forces at 27° and 45°. At the beginning of the second set of experiments, two different angle conditions were investigated in which tactile display was driven with 4 mm x 4 mm and 4 x 2 mm strokes in X and Y axes, respectively. Exciting the display 4 mm x 4 mm strokes results in 5.65 mm resultant relative displacement at 45 degree while 2 mm x 4 mm strokes results in 4.47 mm resultant relative displacement at 27 degree between the artificial finger and the display. In the first condition, the touch screen was excited with 4 mm strokes in X and Y axes provided by using 2 mm modular crank length apparatus. Since the finger was stationary, two fold of crank length corresponds to the relative displacement between the finger and the touch screen. In the second condition, the touch screen was excited 4 mm x 2 mm strokes in X and Y axes provided by using 1 mm and 2 mm modular crank length components. During the oscillation of the tactile display with electrostatic attraction, the directional force field occurs on the tactile display as illustrated in Figure 3.23.

In addition to electrical signal synchronization, initial crank positions have been kept 0 degree angle before the experiments for the mechanical synchronization. A ruler was attached to the base, and a point on the touch display was tracked to measure displacements. The motion of the display were recorded by a camera and observed for

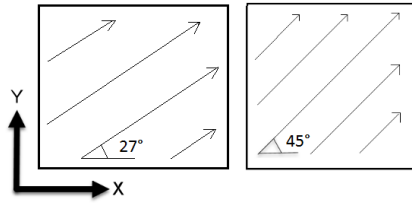


Figure 3.23. Directional force fields at 27 and 45 degree angles.

calibration. The artificial finger is used and electrically grounded in this experiment.

3.2.2.2. Orienting the directional force. In the last experiment, tactile display was continuously and alternately oscillated along five angles from 0 to 180 degree with 45 degree of increments. In order to shift the angle of the lateral force continuously, the step motors drove the tactile display with a new control algorithm written in Arduino Uno. During the experiment, the tactile display was driven only with 4 mm stroke in either single axis or in both X and Y axes. When the experiment began, in the first stage, tactile display moved in X axis corresponding to a force field at 0 degree angle, in the second stage, tactile display moved in X and Y axes after 4 sec corresponding to a force field at 45 degree angle, in the third stage, the tactile display moved in only Y axis corresponding to a force field at 90 degree angle, in the fourth stage, the tactile display moved in X and Y axes with the half revolution delay in X axis in order to obtain force field in 135 degree angle and in the final stage of the experiment, tactile display moved in only X axis corresponding to force field at 180 degree angle. Because of the half revolution delay in X axis created for the fourth stage, the directional force field rotated from 0 to 180 degree angle. During the excitation of the tactile display when there was an electrostatic force, the directional force fields occur on the tactile display as seen in Figure 3.24.

In addition to the signal synchronization, mechanical synchronization was also required before these experiments. The force sensor collected lateral force values for 4 seconds for each angle. The artificial finger was electrically grounded during this experiment.

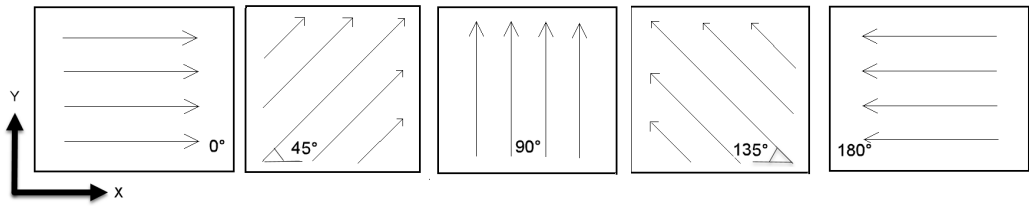


Figure 3.24. Rotated directional force field in sequence.

4. EXPERIMENTAL RESULTS

Two set of experiments have been conducted. For the first set, three experiments were conducted to examine the feasibility of active feedback on the electrostatic tactile display, as explained in Section 3.2.2. For the second set, three experiments were conducted to extend our work for 2-DOF active electrostatic tactile feedback on the tactile display, as explained in section 3.3.2. The results must be evaluated by taking into account the Section 3.1, creating active feedback using electrovibration method.

4.1. Experimental Results of 1D Measurements

4.1.1. Minimum Displacement for Active Feedback

Following the procedure described in Sec. 3.2.2.1, lateral forces were measured for three stroke values. Results are shown in Figure 4.1. The peak value of the lateral friction force is much higher for 4 mm stroke (around 0.3 N) than the others (less than 0.05 N). Also, high-frequency vibrations are seen in the lateral force of 2 mm and 4 mm strokes when there is an electrostatic attraction. Although lateral friction forces were felt in both back and forth movements for 4 mm stroke, the higher lateral force due to the electrostatic attraction was observed only in one-half of the periodic movement, as expected. These results show that while 4 mm of relative displacement resulted in a net directional force of 0.2 N, lower relative displacements did not create any directional force. Therefore, the display was driven at this stroke in the further steps of the experiments.

4.1.2. Effect of Frequency on Directional Force

We have tested four distinct frequencies as explained in Sec. 3.2.2.2. Our hypothesis was that the electrostatic force and hence the resultant directional force increase if the frequency of the excitation signal for electrostatic attraction is increased. Results are shown in Figure 4.2. The dashed black line is plotted as a reference, which is the

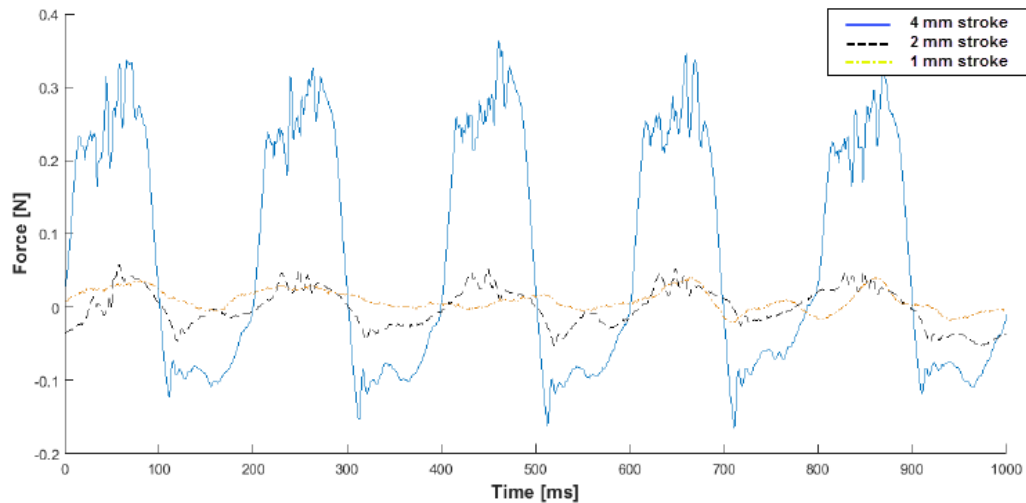


Figure 4.1. Measured lateral forces for three relative displacements when the electrostatic tactile display was driven by a 270 Hz and 397 V_{pp} square wave which was periodically enabled and disabled at 5 Hz. (Bottom) Synchronized input signals.

friction force on the surface without any electrostatic attraction. The mean resultant forces increase from 0.1 N to 0.3 N for the frequencies from 80 Hz to 270 Hz as seen in this figure. This result is consistent with the previously reported results with the passive systems and explained by a simple RC model of the skin and the insulator [29].

Increased lateral force is observed only in one-half of the periodic movement. Besides, the lateral force is equal to the surface friction in the other half of the movement. These show that directional force is obtained with the electrostatic attraction.

4.1.3. Effect of Amplitude on Directional Force

Although it is well known that increasing amplitude of excitation voltage increases electrostatic attraction, we wanted to observe the same behavior in the active feedback case. Following the procedure in Section 3.2.2.3, lateral forces were measured for three different excitation conditions. Results are shown in Figure 4.3. Although the finger was grounded in one of the 215 V_{pp} cases, the mean lateral force is still less than

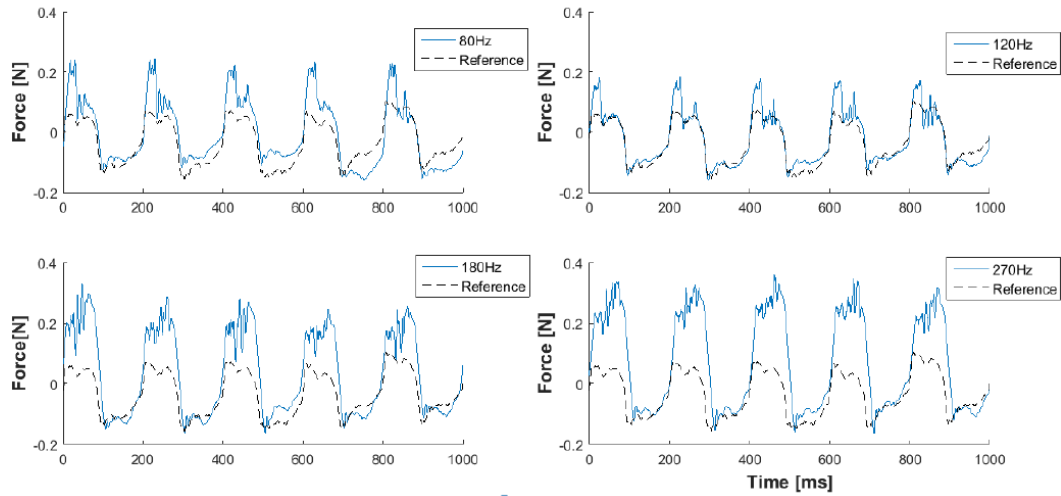


Figure 4.2. Measured lateral forces for four electrostatic excitation frequencies. Blue line represents the condition that $397 V_{pp}$ square wave was periodically enabled and disabled at 5 Hz. The black dashed lines show the measurements when the electrostatic attraction was disabled.

$397 V_{pp}$ when the electrostatics was enabled. Without grounding, the lateral force measurements were much lower for $215 V_{pp}$. Since the mean lateral forces due to the electrostatic attraction are almost equal to the lateral forces when the electrostatics was disabled, we can conclude that directional force is not obtained for $215 V_{pp}$. However, increased lateral force due to the electrostatic attraction is observed for $397 V_{pp}$. This shows that higher voltages are desired to create a directional force.

4.2. Experimental Results of 2D Measurements

4.2.1. Directional Forces at 27° and 45°

The lateral forces were measured for two cases: When the tactile display was excited with a) 4 mm strokes and b) 4 mm x 2 mm strokes in X and Y axes, respectively. The results consist of two parts: First part of the results are collected when there is a half cycle electrostatic attraction, second part of the results are collected when there is not any electrostatic attraction. Figure 4.4 and 4.5 are chosen as representative samples

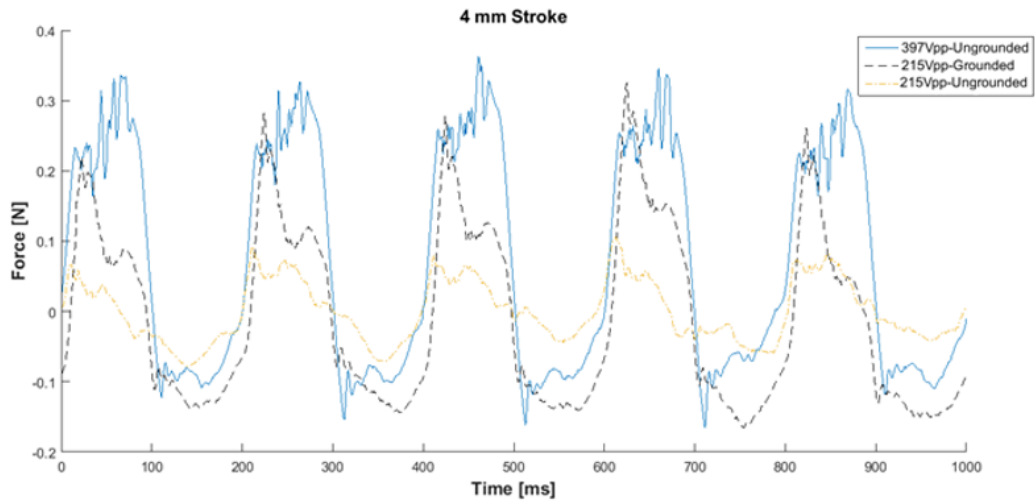


Figure 4.3. Measured lateral forces for three different voltage conditions when the electrostatic tactile display was driven by a 270 Hz square wave, which was periodically enabled and disabled at 5 Hz. The finger was electrically grounded for one of the 215 V_{pp} cases.

of all measurements. The reason why the results have two parts is to observe the instantaneous alteration of directional force. The net directional forces are calculated by, for instance, subtracting the absolute mean lateral forces in X direction from the absolute mean lateral forces in -X direction regarding the first part of the results. In the first case, two step motors drives tactile display in X and Y axes simultaneously providing 45 degree angle with respect to X axis of force sensor. Results are seen in Figures 4.4 and 4.5. The absolute average value of the lateral force in X axis is around 0.22 N and in Y axis is around 0.18 N when there is an electrostatic force. In case that there is not electrostatic force, the absolute average value of the lateral forces are around 0.12 N and 0.08 N in X and Y axes, respectively. Even though bi-directional lateral forces occur in 45 degree angle, the higher lateral force due to the electrostatic attraction is observed only in one-half of the periodic movement. In other half of the periodic movement, lower lateral forces occur, as expected. The net resulted directional forces are 0.1 N in both X and Y axes for 4 mm stroke. Therefore, we can conclude that electrostatic attraction causes 0.1 N increase in lateral force. However, the electrostatic attraction caused 0.2 N increase in the 1D measurements likely due to the different

friction force coefficients and electrical conductivities between the fingertip and the artificial finger. Additionally, the red arrows which shows the difference of black dashed lines corresponding to the average lateral forces with and without the electrostatic attraction inserted in the Figures 4.4 and 4.5. This arrow indirectly represents the amount of the net directional force as well, since the absolute average value of the lateral forces without an electrostatic force in the first part are same with the second part of the results.

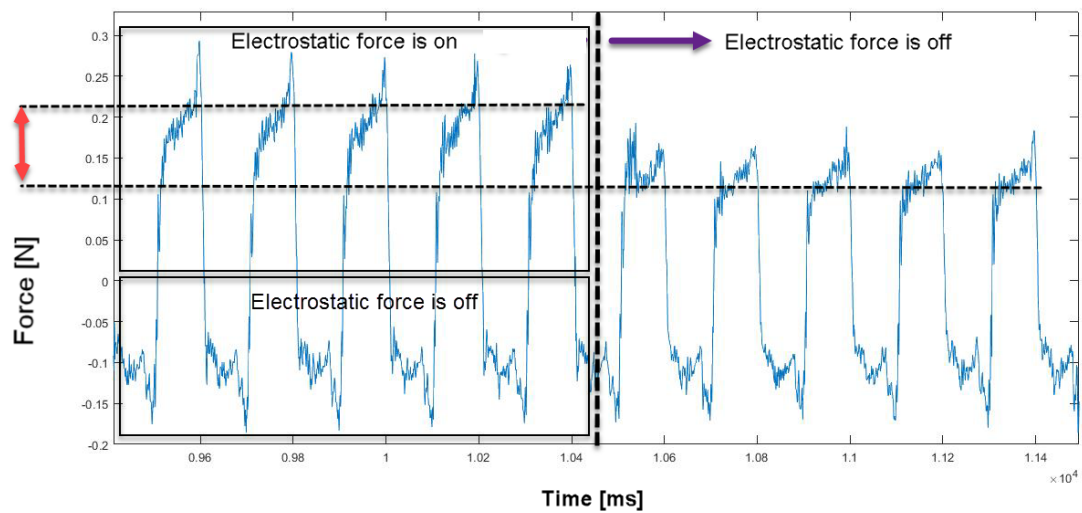


Figure 4.4. Lateral forces measured along X axis when the tactile display was moved with 4 mm stroke. The top rectangular area show the lateral forces with an electrostatic force, while the bottom rectangular area and the rest show the lateral forces without an electrostatic force.

In the second case, the step motors drive tactile display with 4 mm x 2 mm strokes in X and Y axes simultaneously leading to a 27 degree angle with respect to force sensor axis. Force measurements in Y axis are shown in figure 4.6. Due to the amount of net directional force in X axis resulted in the same results of the first case in X axis, the figure 4.5 is valid for the second case as well. The absolute average value of the lateral force is around 0.17 N in Y axis when there is an electrostatic force. In case that there is not electrostatic force, the average value of the lateral force is around 0.12 N in Y axis. The directional force field due to the electrostatic attraction is observed

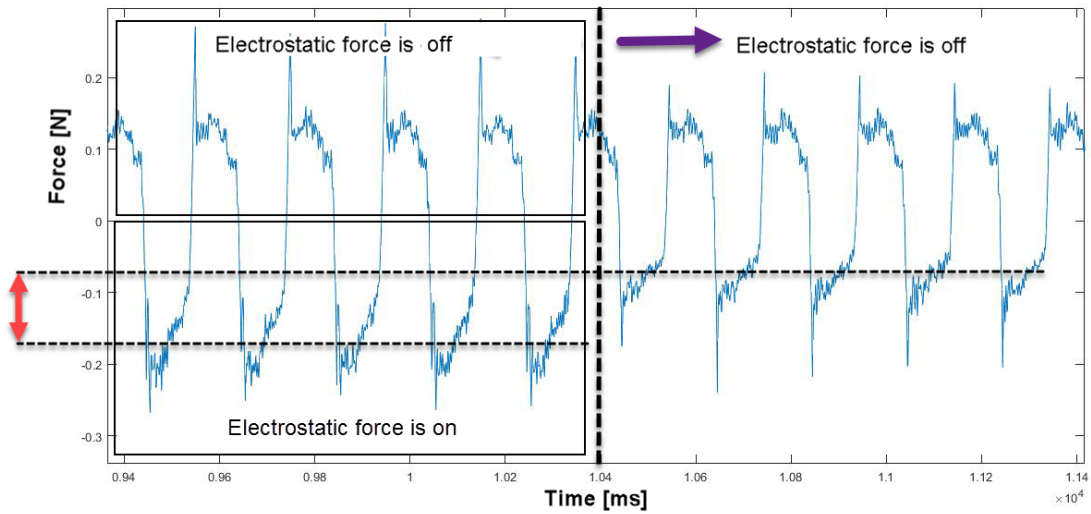


Figure 4.5. Lateral forces measured along Y axis when the tactile display was moved with 4 mm stroke. The bottom rectangular area show the lateral forces with an electrostatic force, while the top rectangular area and the rest show the lateral forces without an electrostatic force.

only in one-half of the periodic movement, as expected, while lateral friction forces are created in 27 degree angle. These results show that 4 mm and 2 mm strokes in X and Y axis resulted in a net directional force of 0.1 N and 0.05 N, respectively. Besides, a low pass filter was applied to the lateral forces measured along X and Y axes for 45 and 27 degree experiments, respectively, in order to introduce the results clearly which are shown in the Figures 4.7 and 4.8.

The measured lateral forces correspond to the friction forces on the tactile display. If the kinetic friction coefficient between the artificial finger and tactile display is assumed to be constant during the experiments, the increase in friction force is because of an expected increase in the contact force due to the electrostatic attraction. In order to calculate the kinetic friction coefficient, equation (4.1) was used. The contact force was assumed to be constant (0.1 N) and the friction force data of the no electrostatic attraction case shown in the black boxes in Figure 4.9 were taken into account. Five boxes at the bottom, which is represented as a subscript of i , were used in the equation. The subscript of j represents the number of force data in boxes, which is 200 for

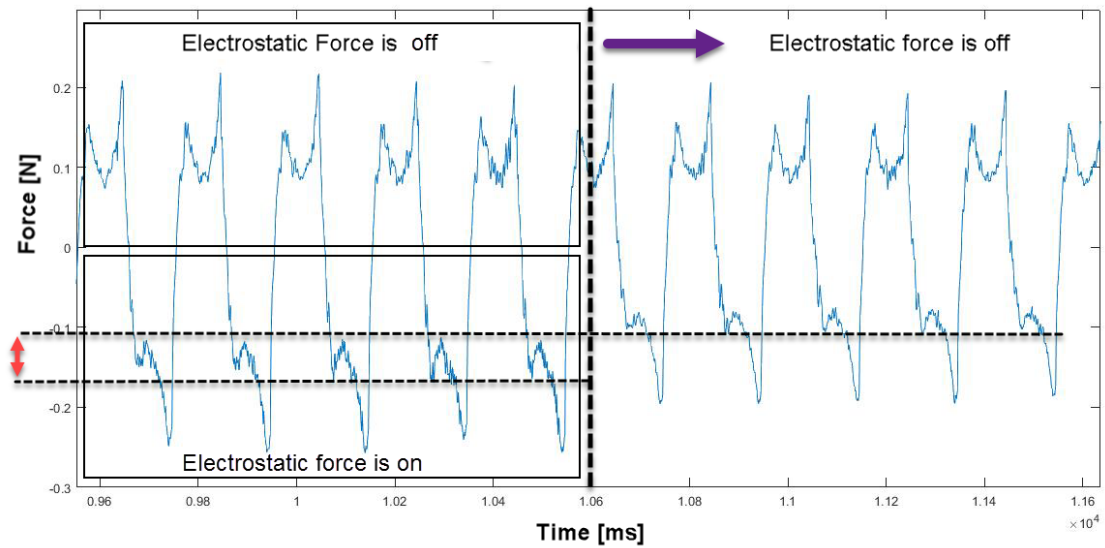


Figure 4.6. Lateral forces measured along Y axis when the tactile display was moved with 2 mm stroke for the 27 degree experiment. The bottom rectangular area show the lateral forces with an electrostatic force, while the top rectangular area and the rest show the lateral forces without an electrostatic force.

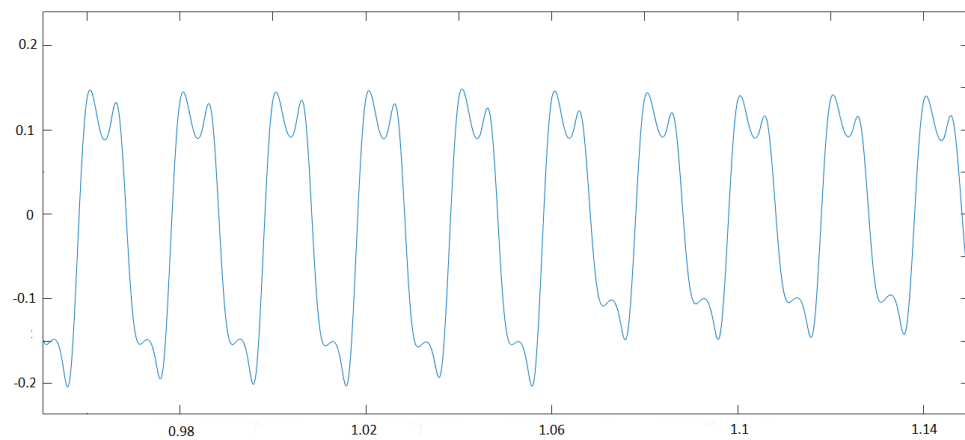


Figure 4.7. Lateral forces measured along Y axis for the 27 degree experiment were passed through a low pass filter with a cut-off frequency of 30 Hz.

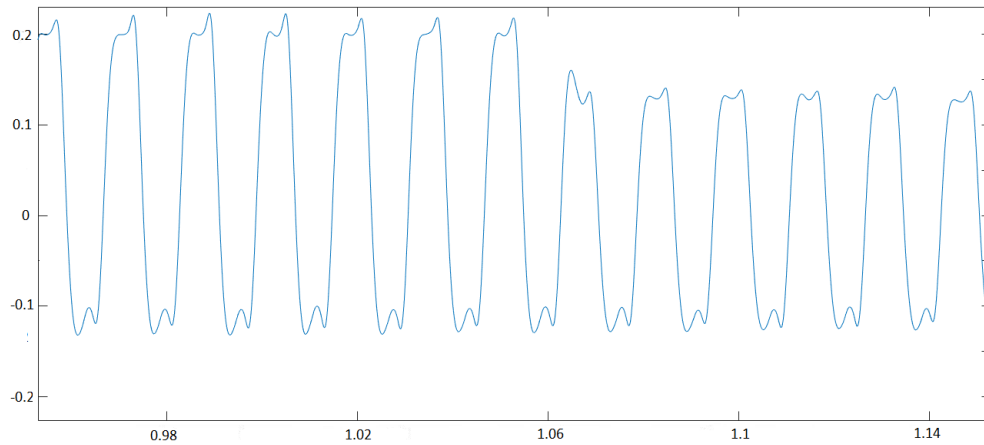


Figure 4.8. Lateral forces measured along X axis for the 45 degree experiment were passed through a low pass filter with a cut-off frequency of 30 Hz.

the equation (4.1). With this method, the kinetic friction coefficient was found to be one. In order to calculate the contact force when there is an electrostatic attraction, the force data in the five boxes at the top shown in Figure 4.9 and the calculated kinetic friction coefficient were accordingly taken into account. The contact force was calculated as 0.2 ± 0.0271 when there is electrostatic force.

$$\mu_k = \frac{(\sum_{n=5}^{i=1} ((\sum_{m=1}^{j=200} F_i(j))/200))/5}{\text{Contact force}} \quad (4.1)$$

Since high-frequency vibrations are observed in the directional force field in both axes, the results are also evaluated in the frequency domain, as well. Force values with and without electrostatic force are separately transformed to the frequency domain as seen in figures 4.10 and 4.11. According to the results, the frequency of excitation signal, 250 Hz, the frequency of excited tactile display, 5 Hz, and the complex harmonic waveforms up to 300 Hz are observed when there is electrostatic force as seen in figure 4.10. These complex harmonic waveforms might be originated from either slider crank

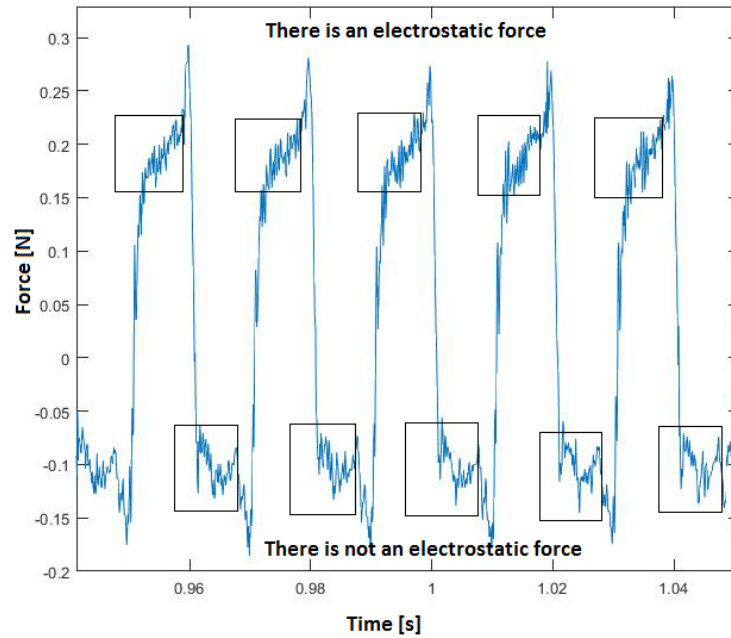


Figure 4.9. Selected areas in order to calculate the two mean kinetic friction coefficients and their standard errors when there is an electrostatic force and not.

mechanism or discontinuous revolutions of stepper motors. As the frequency domain analysis of the slider crank mechanism, which is seen in figure 3.21, is compared with the frequency domain of the measured lateral forces, the complex harmonic waveforms match well up to a 50 Hz. Beyond 50 Hz, the further frequencies occurred with smaller amplitudes, which are likely due to the discontinuous revolutions of stepper motors.

As seen in figure 4.11, the frequency of excited tactile display, 5 Hz and the complex harmonic waveforms up to 300 Hz are observed when there is not electrostatic force. Regarding to these assessments, the directional force field is achieved at 27 and 45 degrees.

4.2.2. Orienting the Directional Force

Following the procedure described in Section 3.3.2.3, the lateral forces were measured during the continuous rotation of directional force field. The tactile display is

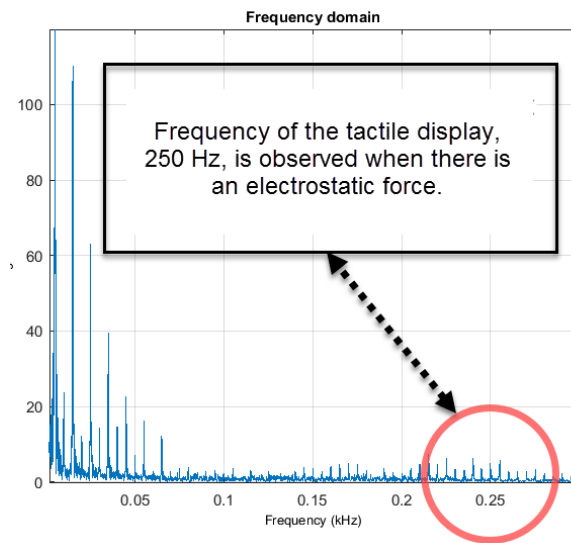


Figure 4.10. Frequency domain analysis when there is an electrostatic force with 4 mm stroke along X axis.

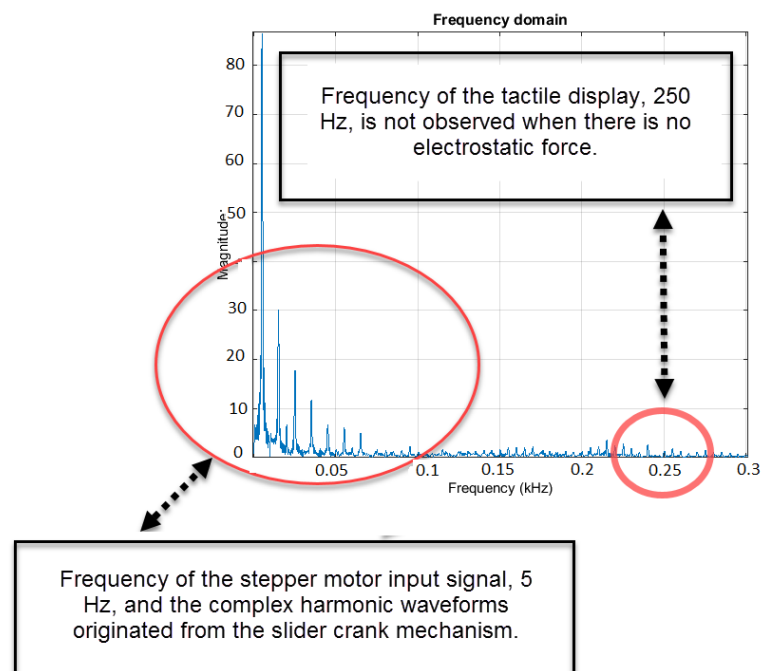


Figure 4.11. Frequency domain analysis when there is not an electrostatic force with 4 mm stroke in X axis.

driven with 4 mm stroke in X or Y axes corresponding to 0, 90, 180 degree angles and 4 mm stroke in both axes corresponding to 45 and 135 degree angles. Experimental results measured in X axis are evaluated based on the figures 4.12 and 4.13. The results measured in X axis are chosen as representative due to the fact that the similar results are obtained in Y axis. At 0 degree angle, the average lateral force is 0.28 N in X direction, while the absolute average lateral force is 0.18 N in -X direction. At 45 degree angle, the average lateral force is 0.22 N in X direction, while the absolute average lateral force is 0.12 N in -X direction. At 90 degree angle, there is not a lateral motion in X axis. At 135 degree angle, the average lateral force is 0.12 N in X direction, while the absolute average lateral force is 0.22 N in -X direction. At 180 degree angle, the average lateral force is 0.18 N in X direction, while the absolute average lateral force is 0.28 N in -X direction. According to the measurements, the net directional force are resulted in 0.1 N by subtracting the force values in X directions from the force values in -X directions.

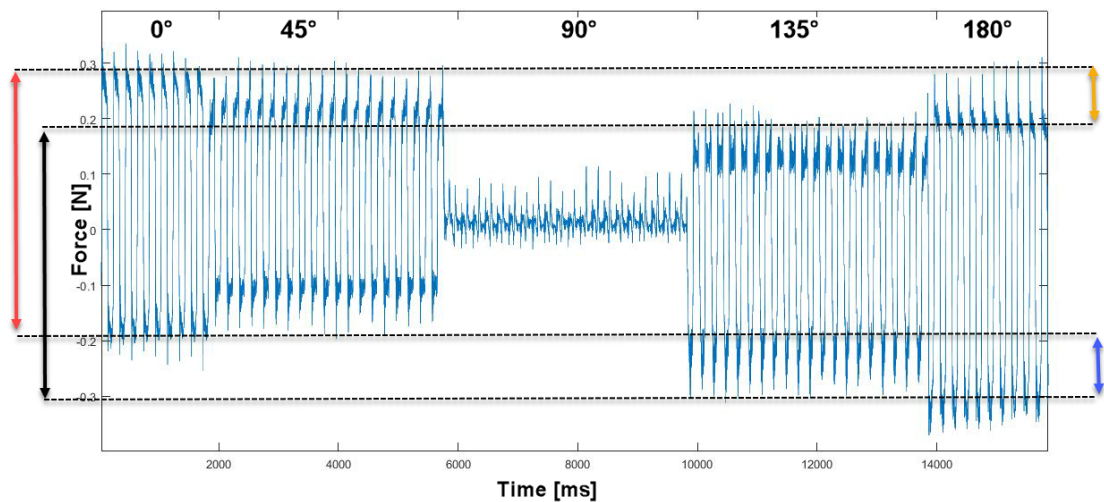


Figure 4.12. Force values measured in X axis at 4 mm stroke when directional force rotates from 0 to 180 degree angles.

Considering figure 4.12, red and black arrows represent the peak to peak lateral force for the motion at 45 and 135 degree angles, respectively, which both are 0.3 N. Orange and blue arrows represents the shifted lateral forces from 45 to 135 degrees, which are 0.1 N. Considering figure 4.13, red and black arrows represent the peak to

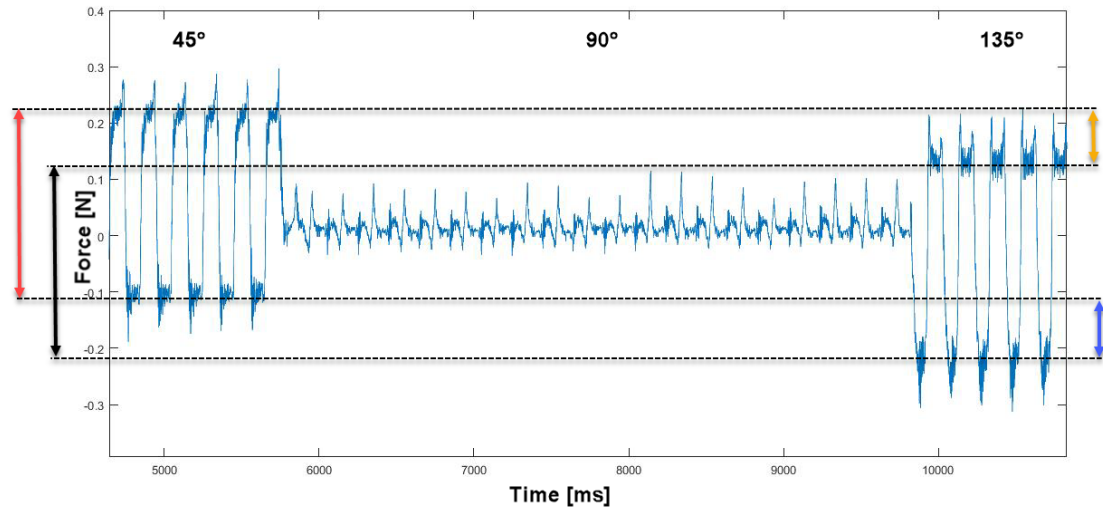


Figure 4.13. Force values measured in X axis at 4 mm stroke when directional force rotates from 45 to 135 degree angles.

peak lateral forces for the motion in 45 and 135 degree angles, respectively, which both are 0.45 N. Orange and blue arrows represents the shifted lateral forces from 0 to 180 degrees, which are 0.1 N. Although the net directional forces are same at each angle, the peak to peak lateral force at 45 and 135 degree are not same with the degrees of 0 and 180. Indeed, this difference occurs because the axes of force sensor were not able to be angled parallel with the direction of excitation of the tactile display at each angle. In other words, the lateral forces at 45 or 135 degree are being a force vector of the actual lateral forces. If that vector is multiplied by $\sqrt{2}$, the actual lateral forces can be found as 0.45 N, and this difference disappears.

5. DISCUSSION

Based on the results analysed in Section 4.1.1, only 4 mm stroke creates a directional force rather than 1 mm and 2 mm strokes, even though the friction force is also felt in the opposite direction of the directional force. A possible reason for this can be the mechanical behavior of the pulp of the finger. In the literature, tangential deformation of the pulp is reported as 3.5 mm for shearing loads of 1.7 N and contact forces of 1.9 N [62]. Besides, according to Wiertlewski and Hayward [63], the partial slip is taking place between the fingertip and a flat surface at the tangential deformation of approximately 2 mm for shearing and contact forces of 0.5 N. In the experiments with 1-DOF mechanism, contact forces are approximately 0.1 N and an anti-static finger cot is worn by the subject for the first set of experiments. These two factors decrease the tangential deformation of the pulp (probably to a value of less than 2 mm) and thus allow slip of the touch screen underneath the finger for 2 mm and 4 mm strokes. In fact, as seen in Fig. 4, high-frequency vibrations in the lateral forces of 2 mm and 4 mm strokes show the electrostatic-induced friction. Assuming that there is no slip for 1 mm, partial slip for 2 mm and complete slip for 4 mm strokes, we can conclude that slip must occur for an active feedback on an electrostatic tactile display. In other words, displacement of the screen must be greater than the deformation of the finger pulp. In fact, our preliminary trials without the finger cot showed that larger displacements were required to create active feedback.

The magnitude of the active force increases while the frequency of the excitation signal for the electrostatic attraction is increased from 80 Hz to 270 Hz. This result is consistent with the previously reported results with the passive systems [29]. Although we investigate the change of friction with respect to frequency, any possible effect of frequency of the input signal on the perceived tactile feeling is not studied.

The well-known proportional relationship between electrostatic-induced friction and voltage amplitude is also demonstrated for active feedback. Our results show that 397 V_{pp} input signal is necessary for a perceivable active force. However, exciting the

tactile display at higher frequencies than 270 Hz are not tried. Active feedback might be achieved with lower amplitudes if the frequency is increased. As demonstrated by Meyer *et al.* [29], increasing frequency of the excitation signal from 100 Hz to 10 kHz increases electrostatic force by two fold.

The second set of experiments are conducted using the same excitation signal, 250 Hz and $397 V_{pp}$, due to the proven results in 1D measurements. Measurements of lateral forces for both the bare finger and the artificial finger are close to each other. Rotating directional force continuously does not allow to adjust force sensor axis angle to be parallel with the axis of motion of tactile display. This issue results in a loss of force measured in the X and Y axes, whereas that force loss occurs due to being force vector with 45 degree or 135 degree angle which disappears if force vector is multiplied by $\sqrt{2}$.

Also, force results of 2D measurements are evaluated in the frequency domain. The aim is to investigate the reliability of experimental results by comparing the frequency responses of the force measurements and the applied signal frequencies. To be able confirm that the system works properly, the frequency of the applied signal should be observed in the frequency domain. According to the results, the frequency of the tactile display oscillation, 5 Hz, and the frequency of electrovibration signal, 250 Hz, are observed in the frequency domain. On the other hand, frequency of 250 Hz is not seen when there is no electrostatic force, as expected. Besides, complex harmonic frequencies of 5 Hz occurs unavoidably in the FFT diagrams maintaining until 150 Hz with decreasing magnitude. To sum up, it is clarified that high frequency fluctuations in the force values occurs due to the excitation signal given to the tactile display.

In Figure 4.2, the measured directional forces have two peaks at each periodic movement for the frequencies of 80 Hz and 120 Hz. On the other hand, this is not clearly observed for the cases of 180 Hz and 270 Hz. Also, in the second set of experiments, there are higher peaks in the measured forces above the average lateral forces whether or not there is an electrostatic force. The reason why there are peaks is likely due to the transition from static to dynamic friction. Since the relative velocity between

the touch screen and the finger is zero at the end of the back and forth movement, the finger was adhered to the touch screen until a slip takes place. This corresponds to the higher peaks in each periodic movement. The relative velocity increases after the slip, thus the dynamic friction increases and forms the latter peaks. The major mechanism of this friction transition is the adhesion which occurred due to the friction coefficient difference between static and dynamic slip conditions on the glass surface. Additionally, although the hysteresis mechanism is considered as the minor mechanism, energy dissipation due to the internal friction of the skin causes non-uniform slip condition which should be investigated in the future.

6. CONCLUSION

In this study, active feedback using electrostatic attraction is investigated progressively using two experimental setups. First, a one dimensional experimental setup is built to analyse three criteria: relative displacement between the finger and the touch screen, frequency and amplitude of the excitation signal for electrostatic attraction. An experimental setup is developed to measure directional forces via a force sensor attached to a finger laterally. Three experiments are performed with different input conditions. The experimental results show that a perceivable directional force is obtained with a square wave of 270 Hz and 397 V_{pp} , which is periodically enabled and disabled while the touch screen is driven back and forth at 5 Hz. Active feedback is practically achieved when the relative displacement is 4 mm, and the lateral force is increased up to two times of the surface friction when the electrostatic attraction is enabled. In other words, slip condition takes place smoothly just in this case rather than the cases of 1 mm or 2 mm. The experiments with lower strokes and lower voltage amplitude do not result in a perceivable active force. We can conclude that slip must occur for an active feedback on an electrostatic tactile display. However, to achieve a slip condition, the relative velocity between the finger and the screen has to be controlled properly. Relative velocity can be altered either by changing the relative displacement or by adjusting the shaker frequency. The latter one is not investigated in this study.

Secondly, two dimensional planar mechanism is developed to extend our work for 2-DOF active electrostatic tactile feedback. This experimental setup is built to measure directional forces in 2 perpendicular axis via a force sensor attached to an artificial finger laterally. Three experiments are performed with the same input conditions, only 2 mm stroke is used in Y axis for the experiment of the directional force at 27 degree exceptionally. These three experiments are conducted using square wave of 250 Hz and 397 V_{pp} in order to obtain perceivable directional forces. Two dimensional active feedback was practically achieved considering the resulted net directional forces. Conducting the experiments of orienting the directional forces provides orienting di-

rectional forces continuously in different angles. The directional forces were created from 0 to 180 degree with 45 degree of increments, and also created in smaller angle, 27 degree.

6.1. Outlook and Future Work

This study experimentally showed that, 2-DOF active feedback can be achieved using electrovibration method. To the best of our knowledge, 2-DOF active feedback had never been demonstrated on an electrostatic tactile display. So far, 1-DOF active feedback has been created using ultrasonic and electrovibration methods. Even though both methods enable active feedback, electrovibration method is more promising procedure than the other due to requiring less energy consumption, being less noisy and working by electrical actuation instead of mechanical actuation. Certainly, there are still concerning matters for electrovibration method which must be solved, such as high voltage requirement, necessity of electrical grounding, deficiency in the literature regarding the static friction between a finger and a surface and relatively high relative displacement requirement.

In order to conduct the experiments for 2D measurements, a planar mechanism was developed based on two slider crank mechanisms, despite the fact that a different mechanism was proposed at earlier stages of this thesis. That mechanism was moving the tactile display by two lever arms positioned in perpendicular with each other. The lever arms actuated by the piezoactuators were used to increase the stroke of the tactile display. However, the experimental results of 1D measurements showed that lever arm mechanism could not reach enough stroke value to create active feedback. Even though slider crank mechanism is easy and reliable method to obtain linear motion, it also has downsides, particularly, due to the inertia of the oscillating parts, high input torque is needed and high stiffness is required at high frequencies. On that account, even if 2-DOF active feedback is achieved by using two slider crank mechanisms at frequency of 5 Hz, one of the parameter, relative displacement, could not be investigated at higher frequencies because of the higher torque requirement. To supply higher torque, stronger and bigger stepper motors must be used, but this leads heavier experimental

setup. On the other hand, complex harmonics beyond 50 Hz which are originated from stepper motor can be avoided by using a DC motor with a high resolution encoder. Even if the experimental setup used in this thesis is designed as small as possible, it is still not applicable for the current electronic devices such as smart phones and tablets due to size and power consumption constraints. However, the current system can be adapted to a relatively bigger touch screen board which can be seen in shopping malls. By this way, a certain store can be found on the touch board by dragging the finger tip to its certain location with the help of active feedback.

For further studies, relative displacement must be investigated to be decreased in order to let this system applicable to the smaller devices. In order to decrease the relative displacement, tactile display should be shaken faster to force the skin get stiffer. A higher stiffness on the fingertip means easier slip condition which would lead to a decrease in the required minimum relative displacement to create active feedback. However, shaking the tactile display faster leads a narrow range to supply an electrovibration signal. In this case, frequency of the excitation signal must be increased which can cause a noise beyond a certain frequency if the tactile display excites faster in order to provide an efficient electrostatic attraction. The artificial finger used at the second stage was performed with the same relative displacement, frequency and amplitude of the excitation signal. Therefore, the artificial finger should be performed with parametric study in the future. Moreover, providing either back or forth motion of the tactile display with different velocities and different type of signal waves to an actuator should be investigated due to the variable friction mechanisms of the skin.

Also, active feedback must be created with less voltage application to tactile display. In order to decrease the amount of voltage requirement, electrical and material properties of the electrostatic tactile display must be improved by producing thinner isolating layer of the tactile display with higher protection from the current flow. Furthermore, the user might be disturbed by the vibrated the tactile display, which also might decrease the image quality of the LCD screen underlying the tactile display. In order to solve these unfavourable issues, the relative displacement between the finger

and the tactile display must be decreased as much as possible.

REFERENCES

1. El Saddik, A., M. Orozco, M. Eid and J. Cha, *Haptics technologies: bringing touch to multimedia*, Springer Science & Business Media, 2011.
2. Orozco, M., A. El Saddik, E. Petriu and J. Silva, *The role of haptics in games*, INTECH Open Access Publisher, 2012.
3. Srinivasan, M. A., “What is haptics?”, *Laboratory for Human and Machine Haptics: The Touch Lab, Massachusetts Institute of Technology*, 1995.
4. Kristoffersen, S. and F. Ljungberg, ““Making place” to make IT work: empirical explorations of HCI for mobile CSCW”, *Proceedings of the international ACM SIGGROUP conference on Supporting group work*, pp. 276–285, ACM, 1999.
5. Isokoski, P., J. Springare and eds., *Haptics: Perception, Devices, Mobility, and Communication: 8th International Conference, EuroHaptics 2012, Tampere, Finland, June 13-15, 2012 Proceedings*, Vol. 7282, Springer, 2012.
6. Radivojevic, Z., P. Beecher, C. Bower, S. Haque, P. Andrew, T. Hasan, F. Bonaccorso, A. C. Ferrari and B. Henson, “Electrotactile touch surface by using transparent graphene”, *Proceedings of the 2012 Virtual Reality International Conference*, p. 16, ACM, 2012.
7. Ilkhani, G., M. Aziziaghdam and E. Samur, “Data-Driven Texture Rendering with Electrostatic Attraction”, *Haptics: Neuroscience, Devices, Modeling, and Applications: 9th International Conference, EuroHaptics 2014, Versailles, France, June 24-26, 2014, Proceedings, Part I*, pp. 496–504, Springer, 2014.
8. Poupyrev, I. and S. Maruyama, “Tactile interfaces for small touch screens”, *Proceedings of the 16th annual ACM symposium on User interface software and technology*, pp. 217–220, ACM, 2003.
9. Dai, X., J. E. Colgate and M. A. Peshkin, “LateralPaD: A surface-haptic device that produces lateral forces on a bare finger”, *2012 IEEE Haptics Symposium (HAPTICS)*, pp. 7–14, IEEE, 2012.

10. Mullenbach, J., D. Johnson, J. E. Colgate and M. A. Peshkin, “ActivePaD surface haptic device”, *2012 IEEE Haptics Symposium (HAPTICS)*, pp. 407–414, IEEE, 2012.
11. Chubb, E. C., J. E. Colgate and M. A. Peshkin, “ShiverPad: A device capable of controlling shear force on a bare finger”, *EuroHaptics conference, 2009 and Symposium on Haptic Interfaces for Virtual Environment and Teleoperator Systems. World Haptics 2009. Third Joint*, pp. 18–23, IEEE, 2009.
12. Mullenbach, J., M. Peshkin and J. E. Colgate, “eShiver: Lateral Force Feedback on Fingertips through Oscillatory Motion of an Electroadhesive Surface”, *IEEE Transactions on Haptics*, 2016.
13. Zhang, Y. and C. Harrison, “Quantifying the Targeting Performance Benefit of Electrostatic Haptic Feedback on Touchscreens”, *Proceedings of the 2015 International Conference on Interactive Tabletops & Surfaces*, pp. 43–46, ACM, 2015.
14. Kim, J., K. J. Son and K. Kim, “An empirical study of rendering sinusoidal textures on a ultrasonic variable-friction haptic surface”, *Ubiquitous Robots and Ambient Intelligence (URAI), 2015 12th International Conference on*, pp. 593–596, IEEE, 2015.
15. Kim, S.-C., A. Israr and I. Poupyrev, “Tactile rendering of 3D features on touch surfaces”, *Proceedings of the 26th annual ACM symposium on User interface software and technology*, pp. 531–538, ACM, 2013.
16. Saga, S. and R. Raskar, “Simultaneous geometry and texture display based on lateral force for touchscreen”, *World Haptics Conference (WHC), 2013*, pp. 437–442, IEEE, 2013.
17. Laitinen, P. and J. Mawnpaa, “Enabling mobile haptic design: Piezoelectric actuator technology properties in hand held devices”, *2006 IEEE International Workshop on Haptic Audio Visual Environments and their Applications (HAVE 2006)*, pp. 40–43, IEEE, 2006.

18. Fukuda, T., H. Morita, F. Arai, H. Ishihara and H. Matsuura, “Micro resonator using electromagnetic actuator for tactile display”, *Micromechatronics and Human Science, 1997. Proceedings of the 1997 International Symposium on*, pp. 143–148, IEEE, 1997.
19. Winfield, L., J. Glassmire, J. E. Colgate and M. Peshkin, “T-pad: Tactile pattern display through variable friction reduction”, *Second Joint EuroHaptics Conference and Symposium on Haptic Interfaces for Virtual Environment and Teleoperator Systems (WHC'07)*, pp. 421–426, IEEE, 2007.
20. Wijekoon, D., M. E. Cecchinato, E. Hoggan and J. Linjama, “Electrostatic modulated friction as tactile feedback: intensity perception”, *International Conference on Human Haptic Sensing and Touch Enabled Computer Applications*, pp. 613–624, Springer, 2012.
21. Robles-De-La-Torre, G. and V. Hayward, “Force can overcome object geometry in the perception of shape through active touch”, *Nature*, Vol. 412, No. 6845, pp. 445–448, 2001.
22. Wiertelwski, M. and J. E. Colgate, “Power optimization of ultrasonic friction-modulation tactile interfaces”, *IEEE transactions on haptics*, Vol. 8, No. 1, pp. 43–53, 2015.
23. Nara, T., M. Takasaki, T. Maeda, T. Higuchi, S. Ando and S. Tachi, “Surface acoustic wave (saw) tactile display based on properties of mechanoreceptors”, *Virtual Reality, 2001. Proceedings. IEEE*, pp. 13–20, IEEE, 2001.
24. Biet, M., F. Giraud and B. Lemaire-Semail, “Implementation of tactile feedback by modifying the perceived friction”, *The European Physical Journal Applied Physics*, Vol. 43, No. 1, pp. 123–135, 2008.
25. Samur, E., J. E. Colgate and M. A. Peshkin, “Psychophysical evaluation of a variable friction tactile interface”, *IS&T/SPIE Electronic Imaging*, pp. 72400J–72400J, International Society for Optics and Photonics, 2009.

26. Yao, H.-Y. and V. Hayward, “Design and analysis of a recoil-type vibrotactile transducer”, *The Journal of the Acoustical Society of America*, Vol. 128, No. 2, pp. 619–627, 2010.
27. Kim, S.-Y. and J. C. Kim, “Vibrotactile rendering for a traveling vibrotactile wave based on a haptic processor”, *IEEE transactions on haptics*, Vol. 5, No. 1, pp. 14–20, 2012.
28. Bau, O. and I. Poupyrev, “REVEL: tactile feedback technology for augmented reality”, *ACM Transactions on Graphics (TOG)*, Vol. 31, No. 4, p. 89, 2012.
29. Meyer, D. J., M. A. Peshkin and J. E. Colgate, “Fingertip friction modulation due to electrostatic attraction”, *World Haptics Conference (WHC), 2013*, pp. 43–48, IEEE, 2013.
30. Giraud, F., M. Amberg, R. Vanbelleghem and B. Lemaire-Semail, “Power consumption reduction of a controlled friction tactile plate”, *International Conference on Human Haptic Sensing and Touch Enabled Computer Applications*, pp. 44–49, Springer, 2010.
31. Marchuk, N. D., J. E. Colgate and M. A. Peshkin, “Friction measurements on a large area TPaD”, *2010 IEEE Haptics Symposium*, pp. 317–320, IEEE, 2010.
32. Bau, O., I. Poupyrev, A. Israr and C. Harrison, “TeslaTouch: electrovibration for touch surfaces”, *Proceedings of the 23rd annual ACM symposium on User interface software and technology*, pp. 283–292, ACM, 2010.
33. Mallinckrodt, E., A. Hughes and W. Sleator Jr, “Perception by the skin of electrically induced vibrations.”, *Science*, 1953.
34. Strong, R. M. and D. E. Troxel, “An electrotactile display”, *IEEE Transactions on Man-Machine Systems*, Vol. 11, No. 1, pp. 72–79, 1970.
35. Agarwal, A. K., K. Nammi, K. A. Kaczmarek, M. E. Tyler and D. J. Beebe, “A hybrid natural/artificial electrostatic actuator for tactile stimulation”, *Microtechnologies in Medicine & Biology 2nd Annual International IEEE-EMB Special Topic Conference on*, pp. 341–345, IEEE, 2002.

36. Grimnes, S., “Electrovibration, cutaneous sensation of microampere current”, *Acta Physiologica Scandinavica*, Vol. 118, No. 1, pp. 19–25, 1983.
37. Fruhstorfer, H., U. Abel, C.-D. Garthe and A. Knüttel, “Thickness of the stratum corneum of the volar fingertips”, *Clinical Anatomy*, Vol. 13, No. 6, pp. 429–433, 2000.
38. Beebe, D. J., C. Hymel, K. Kaczmarek and M. Tyler, “A polyimide-on-silicon electrostatic fingertip tactile display”, *Engineering in Medicine and Biology Society, 1995., IEEE 17th Annual Conference*, Vol. 2, pp. 1545–1546, IEEE, 1995.
39. Vezzoli, E., M. Amberg, F. Giraud and B. Lemaire-Semail, “Electrovibration modeling analysis”, *Haptics: Neuroscience, Devices, Modeling, and Applications: 9th International Conference, EuroHaptics 2014, Versailles, France, June 24-26, 2014*, pp. 369–376, Springer, 2014.
40. Johnsen, A. and K. Rahbek, “A physical phenomenon and its applications to telegraphy, telephony, etc.”, *Electrical Engineers, Journal of the Institution of*, Vol. 61, No. 320, pp. 713–725, 1923.
41. Shultz, C. D., M. A. Peshkin and J. E. Colgate, “Surface haptics via electroadhesion: expanding electrovibration with johnsen and rahbek”, *World Haptics Conference (WHC), 2015 IEEE*, pp. 57–62, IEEE, 2015.
42. Kaczmarek, K. A., K. Nammi, A. K. Agarwal, M. E. Tyler, S. J. Haase and D. J. Beebe, “Polarity effect in electrovibration for tactile display”, *IEEE Transactions on Biomedical Engineering*, Vol. 53, No. 10, pp. 2047–2054, 2006.
43. Giraud, F., M. Amberg and B. Lemaire-Semail, “Merging two tactile stimulation principles: electrovibration and squeeze film effect.”, *World Haptics*, pp. 199–203, 2013.
44. Meyer, D. J., M. Wiertlewski, M. A. Peshkin and J. E. Colgate, “Dynamics of ultrasonic and electrostatic friction modulation for rendering texture on haptic surfaces.”, *HAPTICS*, pp. 63–67, 2014.

45. Auvray, M. and C. Duriez, *Haptics: Neuroscience, Devices, Modeling, and Applications: 9th International Conference, EuroHaptics 2014, Versailles, France, June 24-26, 2014, Proceedings*, Vol. 8618, Springer, 2014.
46. Kim, H., J. Kang, K.-D. Kim, K.-M. Lim and J. Ryu, “Method for providing electrovibration with uniform intensity”, *IEEE transactions on haptics*, Vol. 8, No. 4, pp. 492–496, 2015.
47. Tomlinson, S., R. Lewis and M. Carré, “The effect of normal force and roughness on friction in human finger contact”, *wear*, Vol. 267, No. 5, pp. 1311–1318, 2009.
48. Lindner, M., M. Kröger, K. Popp and H. Blume, “Experimental and analytical investigation of rubber friction”, *Safety*, Vol. 200, p. 300, 2004.
49. Persson, B., O. Albohr, U. Tartaglino, A. Volokitin and E. Tosatti, “On the nature of surface roughness with application to contact mechanics, sealing, rubber friction and adhesion”, *Journal of Physics: Condensed Matter*, Vol. 17, No. 1, p. R1, 2004.
50. Comaish, S. and E. Bottoms, “The skin and friction: deviations from Amonton’s laws, and the effects of hydration and lubrication”, *British Journal of Dermatology*, Vol. 84, No. 1, pp. 37–43, 1971.
51. Smith, A., G. Cadoret and D. St-Amour, “Scopolamine increases prehensile force during object manipulation by reducing palmar sweating and decreasing skin friction”, *Experimental brain research*, Vol. 114, No. 3, pp. 578–583, 1997.
52. Schallamach, A., “The load dependence of rubber friction”, *Proceedings of the Physical Society. Section B*, Vol. 65, No. 9, p. 657, 1952.
53. Lewis, R., C. Menardi, A. Yoxall and J. Langley, “Finger friction: grip and opening packaging”, *Wear*, Vol. 263, No. 7, pp. 1124–1132, 2007.
54. Koudine, A., M. Barquins, P. Anthoine, L. Aubert and J. Leveque, “Frictional properties of skin: proposal of a new approach”, *International journal of cosmetic science*, Vol. 22, No. 1, pp. 11–20, 2000.

55. Drahos, P., V. Kutis, J. Dubravsky and T. Sedler, “Design and Simulation of SMA Actuator”, *International Review of Automatic Control*, Vol. 4, No. 4, pp. 588–593, 2011.
56. Söylemez, E., *Mechanisms*, Middle East Technical University, 1979.
57. Benabdallah, H. S., “Static friction coefficient of some plastics against steel and aluminum under different contact conditions”, *Tribology International*, Vol. 40, No. 1, pp. 64–73, 2007.
58. Derler, S., L.-C. Gerhardt, A. Lenz, E. Bertaux and M. Hadad, “Friction of human skin against smooth and rough glass as a function of the contact pressure”, *Tribology International*, Vol. 42, No. 11, pp. 1565–1574, 2009.
59. Gabriel, S., R. Lau and C. Gabriel, “The dielectric properties of biological tissues: II. Measurements in the frequency range 10 Hz to 20 GHz”, *Physics in medicine and biology*, Vol. 41, No. 11, p. 2251, 1996.
60. Gent, A. and A. G. Thomas, “The deformation of foamed elastic materials”, *Journal of Applied Polymer Science*, Vol. 1, No. 1, pp. 107–113, 1959.
61. Wangsness, R. K., “Electromagnetic fields”, *Electromagnetic Fields, 2nd Edition*, by Roald K. Wangsness, pp. 608. ISBN 0-471-81186-6. Wiley-VCH, July 1986., p. 608, 1986.
62. Nakazawa, N., R. Ikeura and H. Inooka, “Characteristics of human fingertips in the shearing direction”, *Biological cybernetics*, Vol. 82, No. 3, pp. 207–214, 2000.
63. Wiertlewski, M. and V. Hayward, “Mechanical behavior of the fingertip in the range of frequencies and displacements relevant to touch”, *Journal of biomechanics*, Vol. 45, No. 11, pp. 1869–1874, 2012.